UNIVERSITY OF NAIROBI

FACULTY OF ENGINEERING

DEPARTMENT OF ELECTRICAL AND INFORMATION ENGINEERING

Performance Analysis of a Novel SSK Sequence Modulation

By

Abdulrahman Abdalla Faris, BSc. EEE (UoN)

A Thesis submitted in partial fulfillment for the degree of Master of Science in Electrical and Electronic Engineering in the Department of Electrical and Information Engineering of the University of Nairobi

June, 2022

DECLARATION

I declare that this thesis is my original work and has not been submitted elsewhere for examination, award of a degree or publication. Where other people's work, my own work has been used, this has properly been acknowledged and referenced in accordance with the University of Nairobi's requirements.

SIGN..... DATE.....30-June-2022

ABDULRAHMAN ABDALLA FARIS
F56 / 9606 / 2018
DEPARTMENT OF ELECTRICAL AND INFORMATION ENGINEERING
FACULTY OF ENGINEERING
UNIVERSITY OF NAIROBI

This thesis has been submitted for examination with our approval as University supervisors:

DR. PETER O. AKUON

SIGN..... DATE.....5-7-2022.....

DEPARTMENT OF ELECTRICAL AND INFORMATION ENGINEERING
FACULTY OF ENGINEERING
UNIVERSITY OF NAIROBI

PROF. ODUOL V. KALECHA

SIGN..... DATE.....6 / 7 / 2022.....

DEPARTMENT OF ELECTRICAL AND INFORMATION ENGINEERING
FACULTY OF ENGINEERING
UNIVERSITY OF NAIROBI

DEDICATION

This work is in memory of my father, *Mr. Abdalla S. Faris*.

ACKNOWLEDGMENTS

All the praises and thanks be to Almighty God, without whom this work would not have even started. I thank Him for allowing me to undertake this course to completion.

I would like to express my heartfelt gratitude to my supervisors, Dr Peter Akuon and Prof Oduol Vitalis, for their direction throughout this research.

I'd also like to thank my entire family, supportive staff, and other students for their blessings and encouragement. My sincere thanks to Mr. Benson Ojwang, my friend and colleague, for his encouragement and guidance.

Last but not least, I would like to acknowledge the African Development Bank and Ministry of Education for allowing me to undertake my study to completion.

Table of Contents

LIST OF TABLE

LIST OF FIGURES

LIST OF ABBREVIATIONS

6G	Sixth Generation
ABEP	Average Bit Error Probability
ACSM	Antenna Code Sequence Modulation
APM	Amplitude / Phase Modulation
ASM	Antenna Sequence Modulation
AWGN	Additive White Gaussian Noise
BEP	Bits Error Probability
BER	Bit Error Rate
BPCU	Bits Per Channel Use
BPSK	Binary Phase Shift Keying
EGC	Equal Gain Combining
ESM	Enhaced Spatial Modulation
FD-IM	Frequency Domain - Spatial Modulation
FS	Fractional Sampling
FSM	Frequency Sequence Modulation
G(PIM)	Generalized Pulse index Modulation
GSM	Generalized Spatial Modulation
GSSK	Generalized Space Shift Keying
IAS	Inter-Antenna Synchronization
ICI	Inter-Channel Interference
IM	Index Modulation
IoT	Internet of Things
LOS	Line of Sight
LSM	Layered Baud Spatial Modulation
M-ASK	M-ary Amplitude Shift Keying
MA-SM	Multiple Active Spatial Modulation
MAT	Multiple Asynchronous Transmission
MIMOME	Multiple-Input-Multiple-Output Multiple-Antenna Eavesdropper
MGF	Moment Generating Function
MI	Mutual Information
MIMO	Multiple-Input Multiple-Output

MISO	Multiple-Input Single-Output
ML	Maximum Likelihood
M-PSK	M-ary Phase Shift Keying
M-QAM	M-ary Quadrature Amplitude Modulation
MRC	Maximum Ratio Combining
MRM	Multiple Rank Modulation
OFDM	Orthogonal Frequency Division Multiplexing
OOK	On-Off Keying
PCSM	Polar Coded Spatial Modulation
PDF	Probability Density Function
PIM	Pulse Index Modulation
QAM	Quadrature Amplitude Modulation
RF	Radio Frequency
RM	Rank Modulation
SC	Selective Combining
SE	Spectral Efficiency
SEP	Symbol Error Probability
SD-IM	Space-Domain Index Modulation
SIM-OFDM	Subcarrier Index Modulation - Orthogonal Frequency Division Multiplexing
SIMO	Single-Input Multiple-Output
SISO	Single-Input Single-Output
SM-MIMO	Spatial Modulation Multiple-Input Multiple-Output
SM	Spatial Modulation
SMTx	Spatial Modulation Techniques
SMX	Spatial Multiplexing
SNR	Signal To Noise Ratio
SqM	Sequence Modulation
SSK	Space Shift Keying
SSK-SqM	Space Shift Keying Sequnce Modulation
SSM	Symbol Sequence Modulation
STC	Space Time Coding
SV	Sample Variance

TD-IM	Time-Domain Index Modulation
V2V	vehicle-to-vehicle
VBLAST	Vertical-Bell Laboratories Layered Space-Time

ABSTRACT

This thesis is concerned with developing a novel way of transmitting information using non-modulated symbols in sequence. In this scheme, which is named Space Shift Keying-Sequence Modulation (SSK-SqM), multiple time-slots are used. This enables the proposed scheme to accommodate the use of an odd number of transmit antennas instead of a multiple power of two in the cutting-edge technology of spatial modulation schemes.

The proposed technique in this thesis is based on a unique sequence of frequency-flat fading channels, on an incoming pattern of information bits. The flat-fading channels transmit data exclusively in the spatial domain. The proposed mapping table for the transmitter is utilized to build a system model equation. The suggested technique additionally incorporates the derived system model equation and a simple maximum likelihood detector. In a single-input-multiple-output (SIMO) setup, a validation framework is established by utilizing the mutual information (MI) and sample variance (SV) criteria. The closed-form theoretical performance framework for noise and flat-fading was then validated with a Monte-Carlo simulation, which was tightly bounded. Simulations were carried out on Octave Software with the use of a signal processing package.

The proposed scheme results show that a sequence of channels can be used as transmit entities in index modulation. At the same time, enjoy the benefits of classical spatial modulation with enhanced information security. The performance of the proposed model was evaluated using bit error performance curves under the Additive White Gaussian Noise (AWGN) channel model in flat-fading channels. Performance curves for the simulated transmission were compared with theoretical bit error rate (BER) curves. The Rayleigh channel was shown to perform better than the Rician when performance curves were compared. This was due to the fact that high scattering of Rayleigh paths contributed to a low probability of error as the paths are used for conveying information. The use of unique pattern assignment in the mapping table also provides some security since the information can only be decoded if the same table is known at the receiver. This was shown by a secrecy rate analysis employing a wiretap model. The proposed model outperformed both the SIMO (Single-Input-Multiple-Output) and classical SSK in terms of secrecy rate. The secrecy enhancement in the SSK-SqM, suits it well in security sensitive scenario / systems such as in military, vehicle-to-vehivle (V2V) communication, as well as space communication system. A reduction of about fifty percent in receiver computational

complexity was achieved in comparison to other state of the art techniques. The proposed model can be generalized to accommodate various sets of receiver antennas in future work, also using generalized fading distribution such as Nakagami-m as transmit entity.

CHAPTER ONE

INTRODUCTION

1.1 Background

The next generation of wireless communication systems has demanded an exponential and immediate demand for high-throughput and low-energy digital transmission techniques, driven by the popularity of mobile terminals and a vast range of data-intensive applications such as Internet-of-Things-related services (IoT) [1].

There are many difficulties in dealing with wireless communication channels, which is the only aspect the design engineer has less control over. In wireless communications, channel-fading refers to the variation that the signal parameters experience due to propagation features of a wireless channel. The numerical data model shows that the instantaneous power received over some time resembles the realizations of random processes. As power intensity varies randomly, it may tends to a negligible level, which in turn the wireless channel undergo a deep fade. The wireless-fading channel's random nature is significantly different compared to a wired channel, which generally modeled as deterministic. In general, wireless propagation fading effects are categorized into three types: large, medium-scale, and small-scale fast-varying path loss. The third kind is represented by a random channel amplitude that follows a Rice distribution if the line-of-sight (LOS) component is present, a Rayleigh distribution if the LOS component is absent, or a Nakagami distribution that can approximate a Rayleigh or Rice distribution. [2], [3]

In wireless communication systems, a technique known as diversity is used to reduce the small-scale fading effect. To put it simply, diversity is achieved by sending many copies of signals over independent resource dimensions in order to reduce the likelihood of a deep fade. The diversity gain, defined as the decaying order of the error probability curve as a function of SNR, quantifies the performance gain associated by a diversity schemes. Diversity schemes can be classified into the following types based on the system resource. [2]- [4]:

- **Time diversity** is accomplished by transmitting numerous copies of the same signal across multiple time slots with independently responding channels.

- **Frequency Diversity** obtained in a system that operates over a wide-band channel (i.e., with a large enough bandwidth) to distinguish different propagation paths.
- **Space diversity** is achieved by equipping the transmitter and receiver with multiple antennas.

When multiple antennas are positioned at the transmitter, a technique called transmit diversity is typically used to achieve diversity gain via a method called space-time coding (STC). On the other hand, if the receiver has many antennas, the diversity gain can be accomplished using combining strategies such as maximum-ratio, equal-gain, or selection combining, i.e., MRC, EGC and SC. These are termed as receive diversity techniques.

Naturally, both the transmitter and receiver can utilize multiple antennas, a system with multiple inputs and multiple outputs (MIMO) is constructed. The advantage of a MIMO system over a single-antenna system is that it can increase the capacity of a wireless connection without increasing the required bandwidth. The more antennas a transmitter/receiver has, the more signal paths are possible. The higher the data rate and link reliability, the better. V-BLAST (Vertical Bell-Labs Layered-Space-Time) is a well-known application of this MIMO strategy. This technique demultiplexes a data-stream into multiple individual streams known as sub-streams for transmission over a network with multiple transmit antennas. However, implementing this technique provides a difficulty in terms of mitigating inter-channel interference (ICI) and guaranteeing inter-antenna synchronization (IAS) across data-streams sent by separate transmit antennas. Additionally, this scheme necessitates a high level of decoding complexity at the receiver. More importantly, V-BLAST cannot achieve the transmit-diversity gain.

Spatial modulation (SM) has been presented as an enhanced and more versatile solution to typical MIMO communication [5], [6]. Unlike a standard MIMO communication system, which broadcasts multiple data-streams over all existing antennas, SM in MIMO (SM-MIMO) exclusively transmits across a selection of available antennas. As a result of the limited quantity of data streams, ICI as well as IAS are either eliminated or drastically suppressed. A distinguishing feature of SM is the ability to send additional information bits by appropriately indexing (i.e., switching) between antenna subsets. SM-MIMO's spectral efficiency will be

more than one symbol per channel when this feature is used. SM-MIMO is able to attain both spatial-multiplexing as well as transmit-diversity gains associated with typical MIMO communications, but only having a few (or possibly a single) active broadcast antenna at any given modulation time frame. [7]. By employing a limited number of RF path chains, signal processing and circuitry design complexities are reduced considerably, hence increasing the energy efficiency of the communication system. [8]. Energy efficiency, along with spectrum efficiency, has been identified as a critical performance indicator for driving the design and optimization of next-generation wireless transmission systems and protocols. In essence, energy efficiency quantifies the throughput per unit of energy by explicitly considering energy consumption and the complexity of the system. [9]. Recent analytical and modeling studies reveal that SM-MIMO approaches are capable of outperforming a variety of state-of-the-art MIMO schemes. The transmitter must have a sufficient number of antenna components, but only a few must be active at the same time under this design. [10].

Among many systems, Spatial Modulation techniques (SMTs), which is an Index Modulation (IM) in Spatial Domain (SD-IM), has been envisaged as one feasible digital modulation method to suit future technology demands [11].

SSK is a low-complexity variant of SD-IM due to its uniqueness in conveying information using only spatial domain, thus low-complexity at the receiver as only channels are required to estimate the transmitted information, this is the primary advantage of SSK, but at the expense of lower data rate when compared to other SMT's. The proposed technique in this thesis was able to boost the data rate of SSK while retaining the beneficial aspects of traditional SSK.

1.2 Problem statement

New applications like IoT imply skyrocketing in the number of wirelessly connected terminals. Studies forecast that about 11.6 billion connected devices by next year [12] that have to comply with next-generation wireless standards. Consequently, this necessitates better efficiency in the spectrum and energy use, low cost, and improved reliability [13].

Spatial, Frequency and Time-Domain techniques use antennas, sub-carrier, and time-slots, respectively, as transmitting entities. These techniques have demodulation complexity, receiver errors, and low data rates that do not vary linearly with the number of transmitting entities in

SM [11]. This work opts to provide an alternative way of spatial modulation transmission by using channels only in a unique sequence of patterns, i.e., channels as transmit entities.

1.3 Objective

To formulate a digital modulation scheme based on SSK in Sequence Modulation (SqM).

1.3.1 Specific Objectives

i) To Model Gaussian Channels as a transmitting entity in sequence modulation (SqM).

ii) To Simulate and validate the proposed Model under different SNR for BER.

iii) To analyze the secrecy rate and receiver computational complexity of the proposed model.

1.4 Justification

MIMO configuration schemes pose a lot of challenges due to inter-channel and inter Antenna synchronization. The proposed modulation system can eliminate these drawbacks due to the use of channels to convey information. With SqM in IM and flat-fading channels implementation, this thesis is geared towards reducing receiver computational complexity, increase data rate and enhace security by using channels in sequence for information transmission. This model can transmit 4 bits of incoming information, use an odd number of transmit antennas, achieving data rate $\frac{2}{N_\tau}\log_2(N_\tau+1)$ and increase data rate compared to classical SSK ($\lfloor \log_2 N_t \rfloor$), where N_τ and N_t are number of time-slot and antenna respectively. For the same transmit antennas (say 3 antennas) SSK-SqM achieved 1.333 bpcu while SSK 1 bpcu.

1.5 Scope of Work

This thesis focused on developing a novel transmission scheme based on SSK in SqM. The channel considered in this scheme is Rayleigh and Rician Flat fading with added white Gaussian noise (AWGN). The Modeling is done on Octave and Signal Processing package. Three sequences of channels in three-time slots were used to transmit four bits of information. Decoding at the receiver was done when all three-time slots were received.

1.6 Thesis Organization

The rest of the thesis sections are set up as follows: Literature review, system model, and theoretical system model equation in chapter 2, chapter 3 is the methodology, while chapter 4 is the results and Analysis, and chapter 5 is the conclusion and recommendations. Finally, the references used are listed and Appendices, published papers, and similarity index report are attached.

CHAPTER TWO

LITERATURE REVIEW

2.1 Introduction

This segment discusses the required as well as necessary background to understand the developed modulation scheme. The first section describes the basic wireless transmission system. The system's building blocks are described, including digital modulation schemes, channel models, fading, and modulation and demodulation schemes. The following section presents multi-antenna wireless transmission systems—MIMO system configurations. Next, the classical SM system and its variants are presented for a frequency-flat fading channel, and their merits and demerits are conferred. This section is dedicated to discussing spatial modulation techniques (SMTs) and their variants, as the proposed scheme is based on them. Finally, the proposed scheme mapping table, system model, and its ABEP closed-form equation were formulated.

2.2 Digital Communication System

Digital communication, as defined in [14], is concerned with the transmission of information using finite symbols during a finite time interval. The Figure 2.1 depicts a functional setup and elements of digital-communication system. Each block's function is outlined below:

- **Information Source**: Generates an analog / digital information signal for broadcast.
- **Encoder**: is in charge of decreasing redundant information so that it could be rendered at the lowest bit rate feasible.
- **Mapping**: The mapping block is capable of translating a set of bits into series of values that relate towards the modulated signal's low-pass analogous form.
- **Modulator**: The block gives the signal characteristics that make it much more appropriate for transmission across a specific physical link.
- **physical medium**: It is the medium that connects the transmitter and receiver and can sometimes be air, vacuum, copper / coaxial cable, as well as an optical fiber.
- **Detection**: The detection block is in charge of retrieving the signal's so-called decision variables.

- **Decision and De-mapping**: Translates the decision bits variables to estimated bits as well as other relevant variables for processing by the channel decoder block, allowing for the detection and correction of some bit errors.

- **Information sink**: The estimated data bits that result are conveyed towards the destination and information sink.

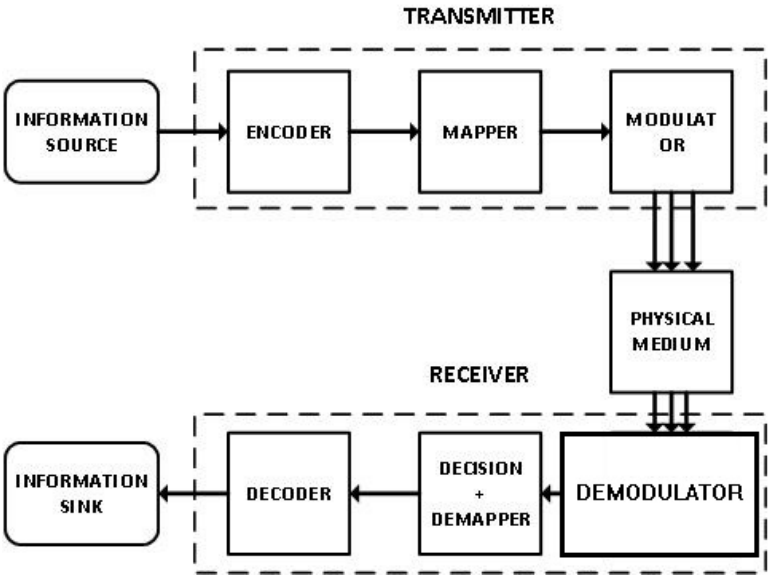

Figure 2.1: Digital Communications System

2.3 Modulation Schemes

A modulator is vital to convey information over a communication network. In BPSK, binary data are denoted by two signals with two angles, 0 and π. The signals are:

$$g_1 = G\Re\{\exp(j2\pi f_a T)\} \tag{2.1}$$

$$g_2 = -G\Re\{\exp(j2\pi f_a T)\} \tag{2.2}$$

The equations 2.1 and 2.2 represents signals known as antipodal. The BPSK has better performance over Amplitude, Frequency, and Phase-Shift Keying techniques in the additive noise. Correlation coefficient of g_1 and g_2 is minus one, which results in a negligible error probability. The BPSK has outstanding noise resistance in contrast to other schemes [15].

BPSK signals can be represented graphically by symbol points in the x-y coordinates system with,

$$\varphi_1 = \sqrt{\frac{2}{T}}\cos(2\pi f_a T) \tag{2.3}$$

$$\varphi_2 = -\sqrt{\frac{2}{T}}\cos(2\pi f_a T) \tag{2.4}$$

as its x and y axis, respectively. The constellation of BPSK is shown in Figure 2.2 where g_1 and g_2 are represented as points on the x-axis with Energy, E as,

$$E = \frac{G^2 T}{2}$$

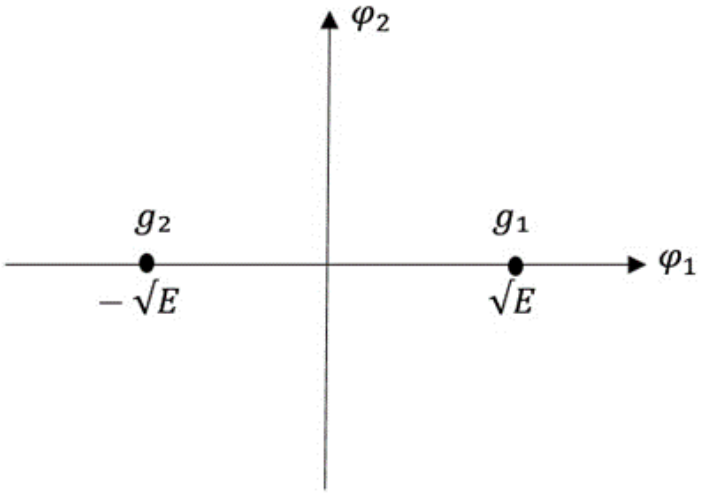

Figure 2.2: BPSK Constellation points

2.3.1 BPSK Modulator

The modulator which generates BPSK is given in Figure 2.3, binary data sequence $\beta(t)$ is formed from the binary data sequence,

$$\beta(t) = \sum_{n=-\infty}^{\infty} \beta_n p(t - nT) \tag{2.5}$$

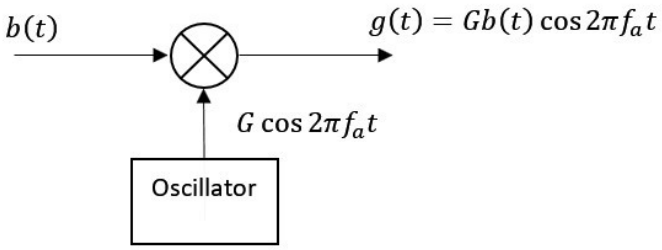

Figure 2.3: BPSK Modulator

where $\beta_n \in \{+1, -1\}$ and $\beta(t)$ is a unit pulse on the range $[0, T]$. The BPSK signal is then given as,

$$g(t) = G\cos(2\pi f_a t) \sum_{n=-\infty}^{\infty} \beta_n p(t - nT) \tag{2.6}$$

$$g(t) = G\beta(t)\cos(2\pi f_a t), -\infty \leqslant t \leqslant \infty \tag{2.7}$$

2.3.2 Additive White Gaussian Noise (AWGN)

Communication system channel paths are not free of disturbances; the prevalent one is thermal noise. Thermal noise P_N is random, and its maximum power transfer depends on temperature T and frequency range ΔF, as related below [16],

$$P_N = KT\Delta F \tag{2.8}$$

The Model used for thermal noise is AWGN, which has a Gaussian-distribution amplitude. Model is presented in Figure 2.4, the received information-bearing signal in the range $[0, T]$ is denoted as,

$$g'(\tau) = g(\tau) + \eta(\tau)$$

where $\eta(\tau)$, - modeled noise process, $g\,(\eta)$- transmitted signal, $g'\,(\eta)$-received signal. As noise is added to the received signal, the probability density function has a Gaussian distribution [17], given as,

$$p(\eta) = \frac{1}{\sqrt{2\pi\sigma^2}} \exp\left(-\frac{(\eta - \mu)^2}{2\sigma^2}\right) \tag{2.9}$$

with $\mu = 0$ and $\sigma^2 = \frac{N_0}{2}$, where N_0 is spectral density.

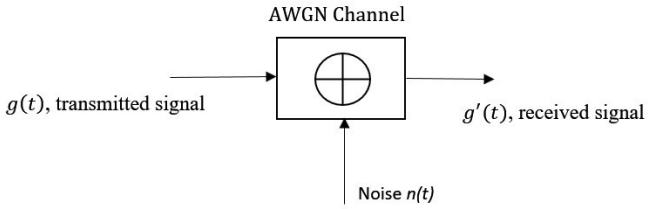

Figure 2.4: AWGN Model

2.3.3 Bit Error Rate (BER)

The system performance of a communication model depends on BER. Transmitted signal is related to noise by SNR performance parameter. SNR and BER are inversely related. Figure

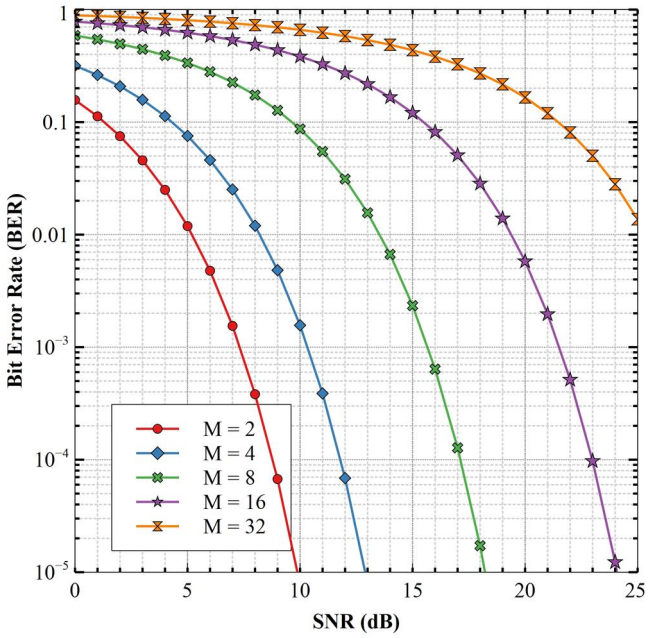

Figure 2.5: Probability of BER for M-PSK

2.5 depicts the theoretical performance curve of BPSK over AWGN. BER curves reveal the behavioral nature of the system [18]

2.3.4 Quadrature amplitude modulation (QAM)

QAM belongs to amplitude-varying scheme with increased efficiency bandwidth than M-PSK with the same energy [19]. QAM modulations alter the phase as well as amplitude of the signal. The symbol constellation points are scattered in the complex-plane with variable energies. In QAM, a signal trait of the carrier is used in the M-ASK amplitude and M-PSK phase to send information. QAM modulated signal is given as;

$$g(\tau) = G\cos(2\pi f_a t)\sum_{n=-\infty}^{\infty}\beta_n p(\tau - nT) - G\sin(2\pi f_a t)\sum_{n=-\infty}^{\infty} a_n p(\tau - nT) \tag{2.10}$$

An M-QAM modulation is systematic if β_n and a_n are equivalent, then the states are a complete square, with M^2.

2.3.5 QAM Constellation

For M-ary square QAM, its signal can represent a linear combination with the following form,

$$g_i(\tau) = I_i\sqrt{\frac{E_0}{2}}\varphi_1 + Q_i\sqrt{\frac{E_0}{2}}\varphi_2 \tag{2.11}$$

(I_i, Q_i) pairs of independent integers that locates symbol point in the array of constellation map, $\min(Ii, Qi)$ are $[\pm 1, \pm 1]$. (I_i, Q_i) is an entry in a $K \times K$ matrix, given by equation 2.12, where $\Gamma = \sqrt{M}$ and M -modulation order.

$$\begin{bmatrix} (-\Gamma+1, \Gamma-1) & (-\Gamma+3, \Gamma-1) & \cdots & (\Gamma-1, \Gamma-1) \\ (-\Gamma+1, \Gamma-3) & (-\Gamma+3, \Gamma-3) & \cdots & (\Gamma-1, \Gamma-3) \\ \vdots & \vdots & & \vdots \\ (-\Gamma+1, -\Gamma+1) & (-\Gamma+3, -\Gamma+1) & \cdots & (\Gamma-1, -\Gamma+1) \end{bmatrix} \tag{2.12}$$

As an illustration, consider 4-QAM, with $M = 4$ and $\Gamma = 2$, hence the matrix becomes,

$$\begin{bmatrix} (-1, 1) & (1, 1) \\ (-1, -1) & (1, -1) \end{bmatrix} \tag{2.13}$$

Figure 2.6 [3] shows a constellation map for 4-QAM and 16-QAM. The symbol point can readily be found from equation 2.12 as stated by [19]

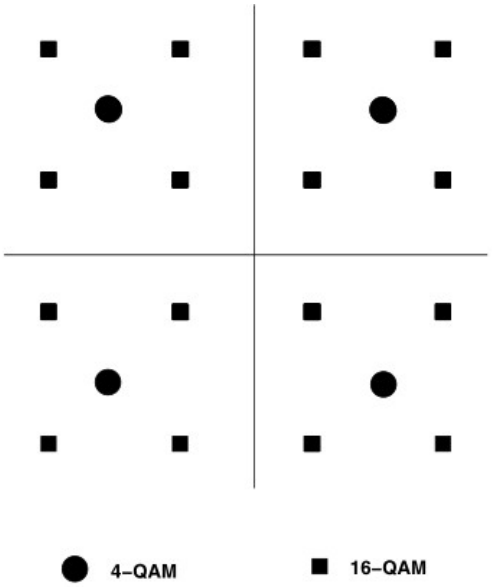

Figure 2.6: 4-QAM and 16-QAM constellations

2.3.6 Theoretical Symbol Error Rate - BPSK and 4QAM

Probability error for MQAM is given as [20],

$$P_{MQAM} = 4\left(\frac{\sqrt{M}-1}{\sqrt{M}}\right)Q\left(\sqrt{\frac{3}{M-1}\gamma}\right) - 4\left(\frac{\sqrt{M}-1}{\sqrt{M}}\right)^2 Q^2\left(\sqrt{\frac{3}{M-1}\gamma}\right) \tag{2.14}$$

where $Q(\bullet)$ is defined as $Q(\hbar) = \frac{1}{\sqrt{2\pi}}\int_{\hbar}^{\infty}\exp(-\frac{x^2}{2})dx$ and known as Q-function, γ is SNR measured at the receive side [21]. The probability error for BPSK ($M = 2$) and 4-QAM ($M = 4$) can be found as,

$$P_{BPSK} = Q\left(\sqrt{2}\gamma\right) \tag{2.15}$$

$$P_{4QAM} = 2Q\left(\sqrt{\gamma}\right) - Q^2\left(\sqrt{\gamma}\right) \tag{2.16}$$

These equations give theoretical symbol error probability over AWGN.

2.4 Wireless Communication Channels

Wireless communication systems transmit data via an open-space medium. Data is transmitted into the communication channel via the transmitter, which as an input. The receiver, alternatively referred to as the output, receives the data transmitted from the input. There are

numerous configurations based on the number of receiving and transmitting antennas. There are several configurations available: Single-Input / Single -Output (SISO), which uses one antenna for both the receiver / transmitter, Multiple output - SIMO, Multiple input - MISO, and MIMO.

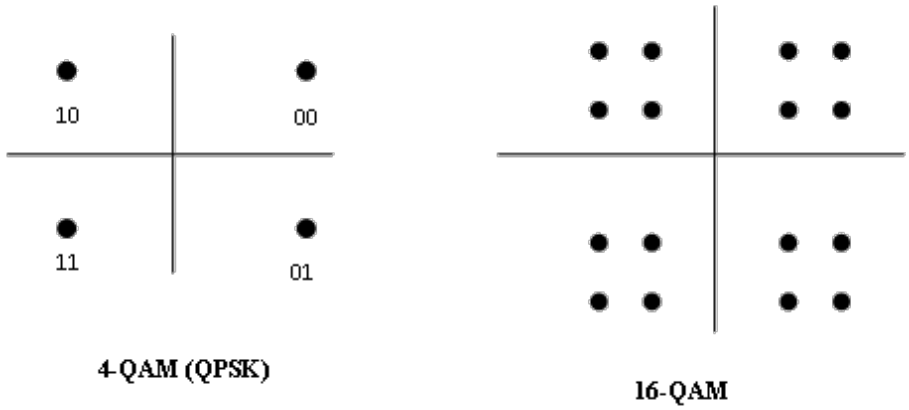

Figure 2.7: 4-QAM and 16-QAM Constellation Map

At transmit, antenna data bits are assigned to symbols based on the modulation technique used. Typically, modulation schemes are depicted as constellation points in a two-dimensional plane, as illustrated in Figure 2.7. The constellation diagram is said to be an M-ary constellation when there are M-mapped symbols on it. For $M = 2^n$ Where n is an integer, then n bits per constellation point. Consider M-QAM with M=4 and M=16 as depicted in Figure 2.7, then the number of bits per constellation point is two and four, respectively.

In communication systems, two items are considered as requirements for bench-marking the quality of service, namely:

1. High Spectral efficiency, and
2. Minimal Bit Error Rate.

It is clear; the first requirement can be achieved by incorporating M-ary schemes shown above since several bits are transmitted per symbol. But this lowers the BER performance because, in higher-order, M-ary constellation points are nearer to each other, hence the high probability of

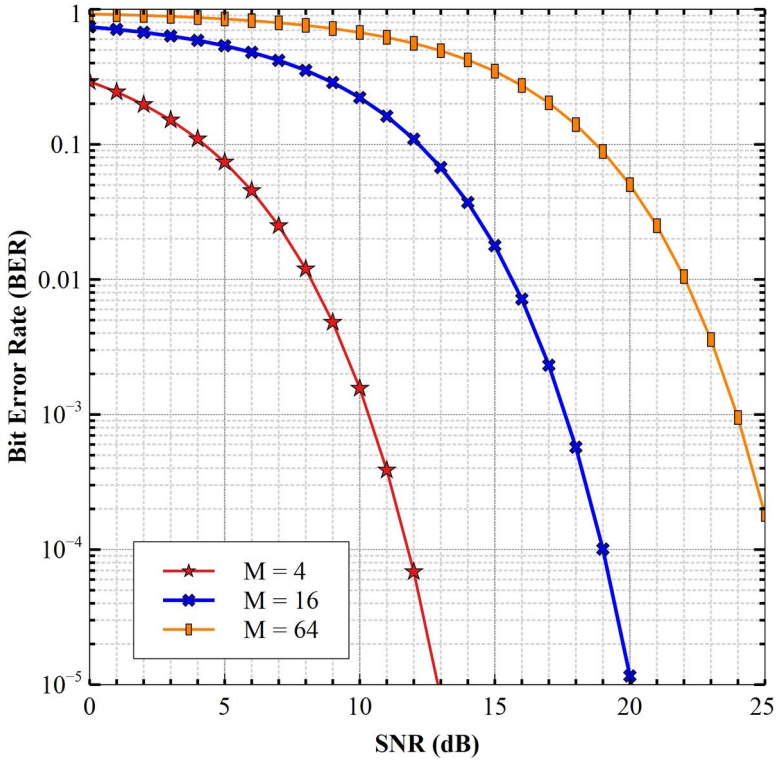

Figure 2.8: BER Comparison for 4, 16, 64-QAM

error in locating transmitted symbol as is shown in Figure 2.8. M-ary schemes exhibit a trade-off performance amongst spectral efficiency and BER metrics [20]. Apart from BER degradation by higher-order M-ary modulation schemes, the environment also plays a significant role in lowering BER performance as the signal undergoes fading phenomena when transmitted in a scattering environment.

2.4.1 Rayleigh Fading

The fading characteristics are channel-dependent. The channel coefficient is treated as a complex random variable whose distribution is determined by the scattering environment's nature for flat-fading channels. Rayleigh, Rician, and Nakagami distributions are all examples of distributions [**?**]. Rayleigh fading is the most severe type of fading that may occur in wireless communication channels. When the received signal is not in Line-of-Sight (LOS), the fading follows Rayleigh distribution, and probability density function (PDF) for the amplitude fading

in Rayleigh distribution is as follows:

$$p_X(x) = \frac{2x}{\Omega} e^{-\frac{x^2}{\Omega}} \tag{2.17}$$

where $\Omega = E(X^2)$ is the fading power. Then SNR is exponentially distributed as,

$$p_\gamma(\gamma) = \frac{1}{\bar{\gamma}} e^{-\frac{\gamma}{\bar{\gamma}}} \tag{2.18}$$

where $\bar{\gamma}$ and γ are the average and instantaneous SNR, respectively. Figure 2.9 shows fading channel model. This Model can be used to understand the effects of fading in a communication channel. The base-band received signal is as,

$$\mathbf{y[i]} = \mathbf{h[i]x[i]} + \mathbf{n[i]} \tag{2.19}$$

Where $h[i] \sim \mathcal{N}(0, \sigma^2)$ are the flat-fading channel coefficient and $n[i] \sim \mathcal{N}(0, N_0)$ AWGN. A

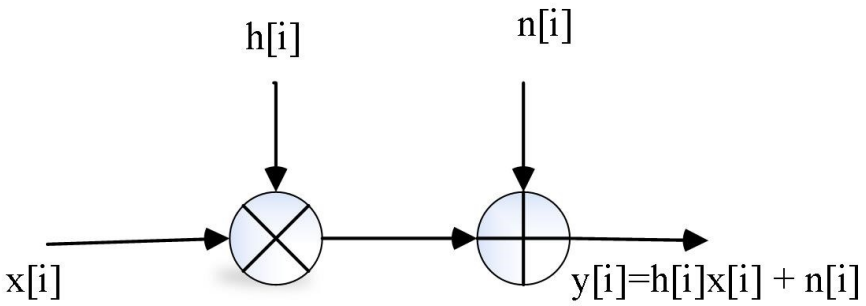

Figure 2.9: Wireless Channel Model

review of the effects of AWGN only is necessary to appreciate the influence of fading. Equation 2.19 without fading as,

$$\mathbf{y[i]} = \mathbf{x[i]} + \mathbf{n[i]} \tag{2.20}$$

For BPSK with mapping of 0 $\longrightarrow$ -A and 1 $\longrightarrow +A$, the ML detection of the system symbol is given as,

$$\hat{x}_i = arg\,|y_i - x_i|\, x[i] \in \{A, -A\} \tag{2.21}$$

And probability error is found to be,

$$P_{eAWGN} = Q\left(\frac{A}{\sqrt{\frac{N_o}{2}}}\right) = Q\left(\sqrt{2.\frac{A^2}{N_o}}\right) \tag{2.22}$$

$$P_{eAWGN} = Q\left(\sqrt{2SNR}\right) \tag{2.23}$$

where $\frac{A^2}{N_o}$ is the average received SNR and $Q(\star)$ is the Q-function defined mathematically as,

$$Q(x) = (\sqrt{2\pi})^{-1} \int_x^{\infty} e^{\left(-\frac{t^2}{2}\right)} dt \tag{2.24}$$

Detection of $x[i]$ from received $y[i]$ for BPSK under flat-fading can be deduced from,

$$\mathbf{r} = \frac{\mathbf{h_i^*}}{|\mathbf{h_i}|}\mathbf{y_i} = |\mathbf{h_i}|\,\mathbf{x_i} + \mathbf{m_i} \tag{2.25}$$

where $m[i]$ follows same distribution as $n[i]$. For channel $h[i]$,probability error is calculated as in AWGN,

$$P_{eRayleigh} = Q\left(\frac{A\,|h\,[i]|}{\sqrt{\frac{N_o}{2}}}\right) = Q\left(\sqrt{2\,|h\,[i]|^2\,\frac{A^2}{N_o}}\right) = Q\left(\sqrt{2.\,|h\,[i]|^2\,SNR}\right) \tag{2.26}$$

For random channel $h[i]$ with $\mathcal{N}(0,1)$, the overall error probability is evaluated by averaging over random gain $h[i]$, which is given [22],

$$P_{eRayleigh} \;=\; E[Q\left(\sqrt{2.\,|h\,[i]|^2\,SNR}\right)] \tag{2.27}$$

$$P_{eRayleigh} = \frac{1}{2}\left(1 - \sqrt{\frac{SNR}{1\;+\;SNR}}\right) \tag{2.28}$$

For high SNR, the error probability is approximated as [23],

$$P_{eRayleigh} \cong \frac{1}{4SNR} \tag{2.29}$$

Figure 2.10 shows BPSK performance over AWGN and Rayleigh fading channel. It can be seen that operating at BER of 10^{-3} requires about 24dB mean SNR, which is much larger than that needed over non-fading Gaussian noise channel, at about 7dB. Equation 2.29 shows that diversity order is one for the system described above, therefore the poor performance of channel because of one link between transmitter and receiver. If it undergoes deep fade, then the transmitted signal will be erroneously detected at the receiver. The Rician fading model is considered in the LOS scenario.

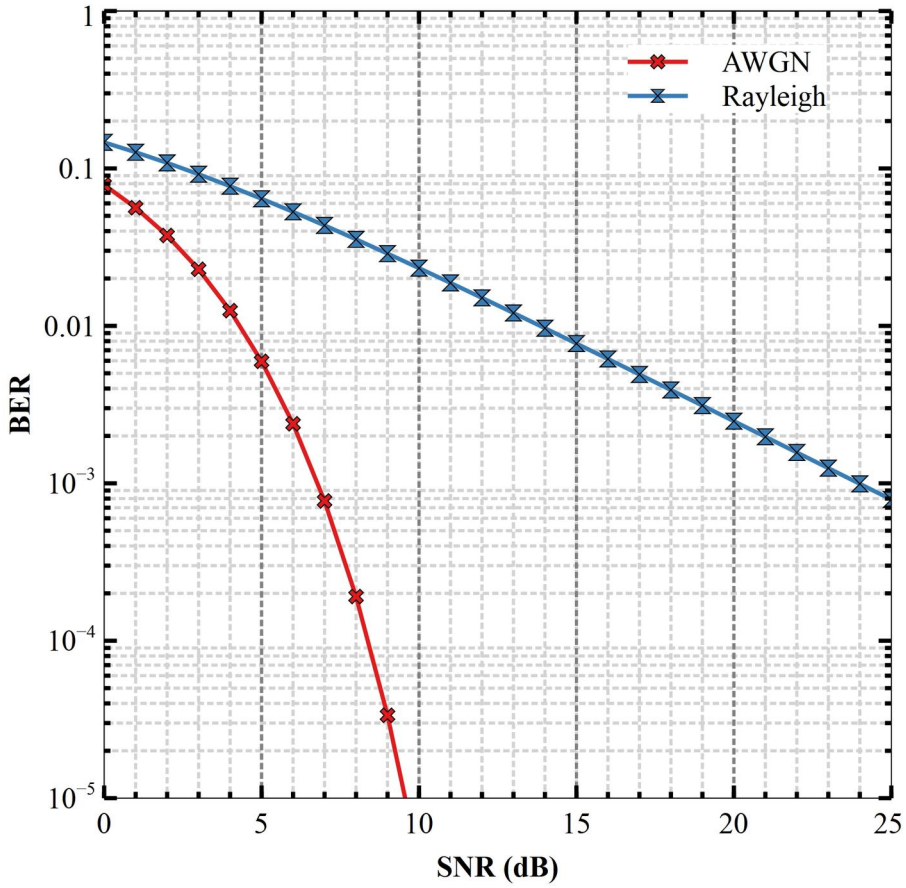

Figure 2.10: BPSK Perfromance

2.4.2 Rician Fading

For the case where LOS exists, i.e., the transmitter and receiver can see each other along the LOS path. For the LOS environment, Rician fading is preferable to characterize channel's amplitude, and the channel thus undergoes Rician fading [18], [22], [24]. Rice distribution is also known as Nakagami-n distribution. The PDF of Rice-distributed amplitude can be given by,

$$p_X(x) = \frac{2(1+\text{K})}{\Omega} x e^{(-\text{K} - \frac{(1+\text{K})x^2}{\Omega})} I_o\left(2x\sqrt{\frac{\text{K}(1+\text{K})\gamma}{\bar{\gamma}}}\right), \gamma \geq 0 \tag{2.30}$$

The PDF of the SNR for which the amplitude is modeled as Rician distributed can be given by,

$$p_\gamma(\gamma) = \frac{(1+\text{Ķ})}{\bar{\gamma}} e^{(-\text{Ķ} - \frac{(1+K)\gamma}{\bar{\gamma}})} I_o\left(2\sqrt{\frac{\text{Ķ}(1+\text{Ķ})\gamma}{\bar{\gamma}}}\right), \gamma \ \geq 0 \tag{2.31}$$

This channel is modeled in MIMO as a sum of LOS and Rayleigh channel matrix components. [18],

$$H_{\text{Rician}} = \sqrt{\left(\frac{\text{Ķ}}{1+\text{Ķ}}\right)}\bar{\mathbf{H}} \ + \ \sqrt{\left(\frac{1}{1+\text{Ķ}}\right)}\mathbf{H} \tag{2.32}$$

The first and second terms in equation 2.32 are the LOS and fading components respectively, where Ķ is referred to as the Rician Ķ factor and is defined as ratio of LOS to scatter power components, $\bar{\mathbf{H}}$ is a unity matrix and $\mathbf{H}$ is an $N_{R_x} \times N_{T_x}$ MIMO channel matrix encapsulates the path gains ($h_{n_{R_x} n_{T_x}}$) between the transmit and receive antennas, and presented as,

$$\mathbf{H} = \begin{bmatrix} h_{11} & \cdots & h_{1n_{Tx}} \\ h_{21} & \cdots & h_{2n_{Tx}} \\ \vdots & \ddots & \vdots \\ h_{n_{Rx}1} & \cdots & h_{n_{Rx}n_{Tx}} \end{bmatrix} \tag{2.33}$$

From no fading (Ķ $= \infty$) to Rayleigh fading (Ķ $= 0$), the Rician fading parameter Ķ can be used to model the channel conditions. Rician distribution can be used to model the fading scenarios when there is LOS and less severe levels of fading.

2.4.3 Correlated Channel Model

The size of the distance between antenna elements has a significant impact on the level of channel correlation. In fact, the correlation magnitude is determined by the signal's frequency / wavelength.

The model developed here is designed for MIMO configuration;, therefore, it is best to consider channel correlation affected by antenna array spacing. For the case of R_x only, the signal correlation for the Rayleigh channel is given as [25]

$$\hat{H} \ = \ R_r^{1/2} \ H_f \tag{2.34}$$

Where: R_r = Spatial Covariance (SC) Matrix at the receiver and H_f = is $N_{Rx} \times \ N_{Tx}$ matrix complex Gaussian coefficients. The correlation coefficients ρ_{mn} between the m^{th} and n^{th}

branches is given as,

$$\rho_{mn} = \frac{E\left[\hat{h}_m \hat{h^*}_n\right]}{\sqrt{\sigma^2{}_{\hat{h}_m}\sigma^2{}_{\hat{h}_n}}} \tag{2.35}$$

Where $\sigma^2{}_{\hat{h}_m}$ and $\sigma^2{}_{\hat{h}_m}$ represent the variance of random variables (RV)'s $\hat{h}_m$ and $\hat{h}_m$ respectively, m,$n = [1, \ldots, N_{Rx}]$. The normalized correlation matrix R can be given as,

$$R = \begin{pmatrix} 1 & \rho_{12} & \cdots & \rho_{1N_{Rx}} \\ \rho_{21} & 1 & \cdots & \rho_{2N_{Rx}} \\ \vdots & \vdots & \ddots & \vdots \\ \rho_{N_{Rx}1} & \rho_{N_{Rx}2} & \cdots & 1 \end{pmatrix} \tag{2.36}$$

In this work, the correlation matrix is assumed to be positive-definite and positive eigen values [26]. Hence correlation coefficients can be found by the Jacobian coefficients of zero-th order of the 1^{st}-kind, i.e., $\rho = J_0\left[2\pi\left(\frac{\delta}{2\nu}\right)\right]$,where δ, ν is antenna spacing and wavelength of the carrier, respectively. For instance, with antenna spacing of $\delta = 0.2\nu$, and for three equally spaced receive antennas, the normalized positive-definite correlation matrix R is given as,

$$\mathbf{R} = \begin{bmatrix} 1 & 0.6425 & -0.055 \\ 0.6425 & 1 & 0.6425 \\ -0.055 & 0.6425 & 1 \end{bmatrix} \tag{2.37}$$

Diversity techniques are used to improve performance without need of increasing power.

2.5 Diversity Techniques

Diversity Strategies use the concept of several copies of received signals due to scattering environments of different strength and nature, and extracting the strongest signal, which improves BER performance. Diversity techniques can utilize time, frequency, and space (Antenna) resources. The first two cost time and bandwidth expansions, while the space diversity technique uses multiple paths (wireless links), hence time and /or bandwidth expansion are not necessary. In the next section, the Diversity schemes and MIMO wireless communication systems are described.

Proper diversity combining schemes can effectively mitigate fading effects on wireless communication. The main idea behind diversity combining is to transmit information signals over several

independent channels – links. By appropriately combining these signal copies, the probability of deep fade is considerably reduced; therefore, improved performance is realised. The channel links or copies of signals can be created using different entities, like, frequencies, time-slots, code words, or even antennas, as stated earlier. The use of antennas to realize diversity is ideal since no spectral resources are required. Figure 2.11 illustrates the general setup of diversity methods.

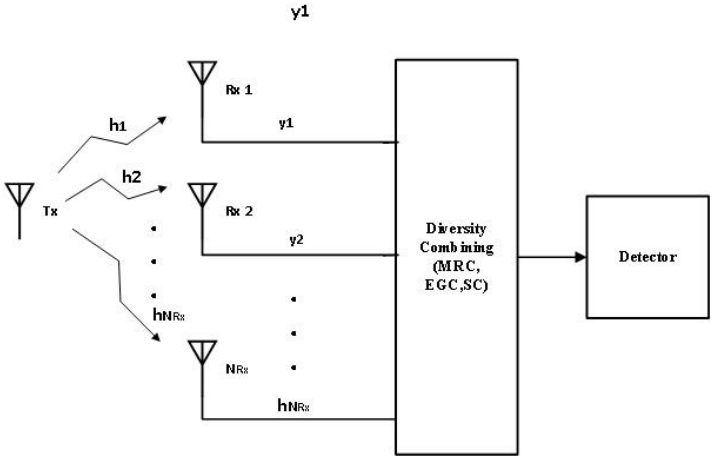

Figure 2.11: Diversity Model

MRC and SC are two commonly used combining techniques, with MRC providing the best performance. The SC scheme has a simple algorithm than the MRC method. However, its performance is lower [20]. Diversity techniques increase diversity order. Figure 2.12 [20] shows a BER performance comparison for BPSK over Flat-Fading Rayleigh channels for several channel links at the receiver. As in Figure 2.12, performance improvement increases as the number of channel link branches added at the receiver increases. It should be noted that the receiver's channel count cannot be increased indefinitely. As a result, the requirement for spectral efficiency (see sec. 2.4) cannot be met. This scenario necessitates several antennas to be used at transmitter in attempt to transmit data concurrently, resulting in transmit diversity. The following section describes the MIMO communication setup, emphasizing its variants for increasing spectral-efficiency and BER performance.

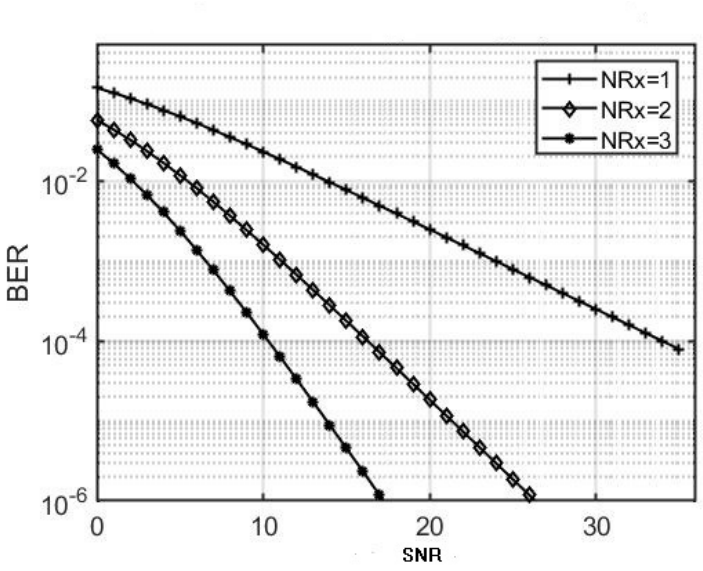

Figure 2.12: BER Performance (BPSK with Fading and MRC Diversity)

2.6 MIMO Wireless Communication System

MIMO technologies include spatial-multiplexing (SMX), space-time block-codes (STBC), and SM. MIMO configuration system in Figure 2.13, where N_{Tx} and N_{Rx} transmit and receive antennas. MIMO system described has a total number of $N_{Rx}N_{Tx}$ paths, with the system

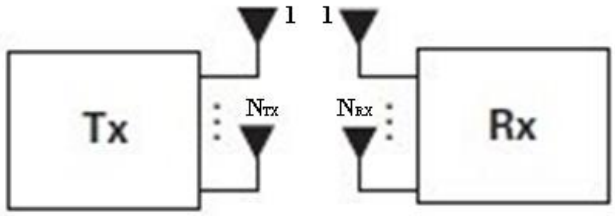

Figure 2.13: MIMO System

described in terms of matrix dimension as $N_{Rx} \times N_{Tx}$ MIMO system. The generalized Model, its channel coefficients, is a matrix of $N_{Rx} \times N_{Tx}$, with the received signal as a vector of $N_{Rx} \times$

1 dimensions. The system can be modeled in matrix form as,

$$\mathbf{y} = \mathbf{H}\mathbf{x} + \mathbf{n} \tag{2.38}$$

SIMO and MISO, are unique categories of MIMO systems. As apparent from the terms, a SIMO system uses multiple receive antennas to provide receive diversity, whereas a MISO system uses multiple antennas at the transmitter to provide transmit diversity. Figure 2.14 illustrates a receiver equipped with N_{Rx} receive antennas to pick up a signal transmitted from a single antenna. The corresponding discrete-time base-band signal at the i^{th} receive antenna for a given time-slot is expressed as,

$$y_i = h_i x + n_i \ , \ i = 1 \dots N_{Rx} \tag{2.39}$$

where x is the symbol transmitted from the digital modulation constellation maps (e.g., M-

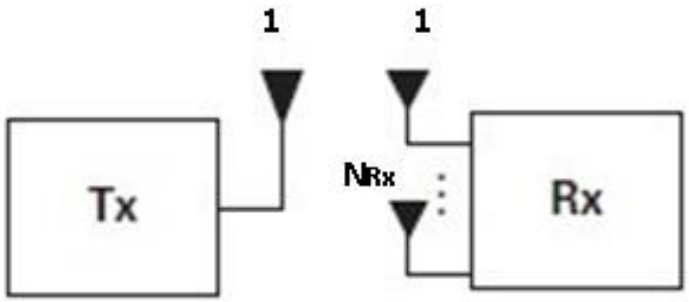

Figure 2.14: SIMO System

QAM), h_i flat fading channel coefficients, and $n_i \sim \mathcal{CN}(0, N_o)$ is AWGN. In matrix form the model is represented as, $y = hx + n$ where $y = [y_1, \dots, y_{N_{Rx}}]^T$, $h = [h_1, \dots , h_{N_{Rx}}]^T$ and $n = [n_1, \dots, n_{N_{Rx}}]^T$.

2.7 Index Modulation

Index modulation (IM) techniques have emerged as an ideal approach for enabling next-generation wireless systems, i.e., 6G [27], because of the agreeable merits of energy and spectral

efficiency specifications, with enhanced BER performance over the traditional digital modulation scheme. IM alleviates the requirement for using all the resources at the transmit side to convey the data message, hence permitting a less complex hardware design at the transmitter. The core principle behind the IM technique is the use of indices of entities at the transmitter like antennas, frequencies, time-slots, and RF mirrors as a means of conveying information. Spatial Modulation (SM), which uses antennas at the transmit side as indices, is a well-known IM application.

2.8 Classical SM and Its Variants

Classical SM concept was introduced by [5], [6]. In addition to traditional Amplitude-Phase Modulation (APM) systems, SM uses index of transmit antenna in a MIMO layout to transmit extra information [6]. The traditional MIMO technologies use SMX and spatial-diversity to improve data rates as well as BER performance and is achieved by conveying different bits from multiple antennae for SMX, and as for spatial diversity, use of multiple copies of symbols [28], [29]. In Classical SM, incoming bits are split into two; one set is used for antenna mapping

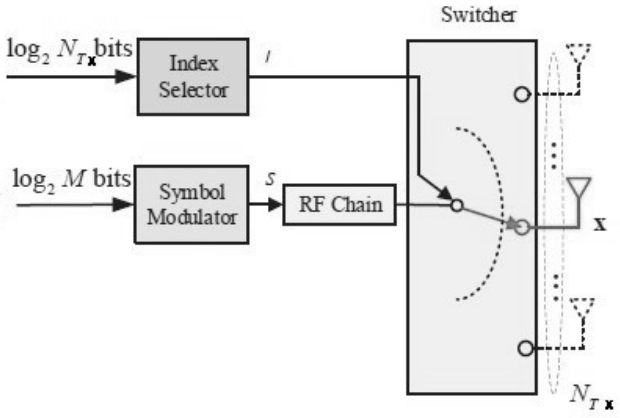

Figure 2.15: Spatial Modulation Transmitter

indexing and second to modulate data symbol by APM as is shown in Figure 2.15 [27], hence for a given transmission, SM ferries two information units, i.e., antenna index and APM symbols, given as

$$\eta_{SM} = \log_2 N_{Tx} + \log_2 M \text{ bpcu-spectral efficiency} \tag{2.40}$$

where bpcu – bits per channel use.

Table 2.1: Example of the SM Mapper Rule $N_{Tx} = 4$ and BPSK

	EXAMPLE OF THE SM MAPPER RULE			
Input bits b	**Antenna bits**	**Antenna index**	**BPSK Symbol bits**	**BPSK Symbols**
000	00	1	0	-1
001	00	1	1	$+1$
010	01	2	0	-1
011	01	2	1	$+1$
100	10	3	0	-1
101	10	3	1	$+1$
110	11	4	0	-1
111	11	4	1	$+1$

Because SM employs only one active antenna in a given time slot, it achieves higher energy efficiency [30], reduces detection complexity, avoids ICI and IAS, and, most importantly, is compatible with conventional MIMO configurations [31]. SM is a superior option to VBLAST [32] due to the advantages listed above.

Two tasks are carried out at SM receiver. Antenna index and APM symbol detection from encoded transmit antenna for demodulation of M-ary symbol constellation. The detection can be achieved by Maximum Likelihood detector where it searches jointly all antenna mapped bits and APM symbol map, leading to search complexity of $(N_{Tx}M)$ [33]. Sub-optimal detector searches the two tasks one at a time, with search complexity of $(N_{Tx} + M)$ [5], [34]. It is seen that there is a noticeable reduction in complexity with a higher number of antenna and high orders of modulation, but error performance is inferior to ML [35]. ML detector will be used in our the proposed Model, since sub-optimal detector is worse in terms error performance compared to ML. Therefore using sub-optimal as a detector can a problem especially for systems that require high performance. Table 2.1 shows a typical mapper rule for four antennas and BPSK as APM scheme.

2.8.1 SSK and G(SSK)

Space Shift Keying (SSK) [36] further reduces detection complexity since it uses only one active antenna to convey information, constellation symbols are not used; hence detection complexity is significantly reduced at the expense of spectral efficiency,

$$\eta_{SSK} = \log_2 N_{Tx} \tag{2.41}$$

since no APM symbols are used in this scheme. Typical Mapper rule for four antennas, is shown in table 2.2. In [37] , generalized SSK (GSSK) has been postulated, in which information is transmitted via several antennas, resulting in a high SE gain but nonetheless a drastic IAS concern. Additional hardware is required to address the IAS issue at the transmitter, whilst SSK does not. The SE for GSSK is given as,

$$\eta_{GSSK} = \left\lfloor \log_2 \binom{N_{TX}}{n_a} \right\rfloor \tag{2.42}$$

where $\lfloor \bullet \rfloor$ and $\binom{\bullet}{\bullet}$ are floor and binomial operator respectively.

Table 2.2: An illustration of SSK Mapper Rule $N_{Tx} = 4$

	EXAMPLE OF THE SSK MAPPER RULE	
Input bits b	**Antenna bits**	**Antenna index**
00	00	1
01	00	2
10	01	3
11	01	4

2.8.2 GSM and MA-SM

One of the flaws of classic SM is that its spectral efficiency is proportional to the logarithm of the number of transmit antennas. Antennas used must be of a factor of power of two. In contrast, VBLAST, SE rises in a linear fashion in relation to N_{TX}, this implies that given the same SE, classical SM would require additional transmit antennas over VBLAST. These obstacles were resolve with the advent of generalized SM (GSM) [38]. Multiple active antennas are utilized in GSM, to transmit the same information, allowing GSM to obtain identical benefits as conventional SM, while improving SE. For the active antenna, say, N_{at}, where $N_{at} < N_{tx}$spectral efficiency for GSM is given as,

$$\eta_{GSM} = \left\lfloor \log_2 \binom{N_{Tx}}{N_{at}} \right\rfloor + \log_2 M \tag{2.43}$$

From 2.43, the SE is better than of SM. ; for instance, if we consider $N_{Tx} = 8$, SM can convey only 3 bits, while GSM with $N_{at} = 4$ can transmit double the number, i.e., 6 bits [35].

The principle of GSM has been generalized to multiple-active spatial modulation (MA-SM) in [39] by conveying different data symbols from various active transmit antennas to increase

spectral. The difference among GSM as well as MA-SM is that in GSM, all enabled antennas transmit the same symbol, whereas in MA-SM, different activated antennas transmit different symbols. As a result, the MA-SM scheme's spectral efficiency is described as

$$\eta_{MA-SM} = \left\lfloor \log_2 \binom{N_{Tx}}{N_{at}} \right\rfloor + N_{at} \log_2 M \tag{2.44}$$

2.8.3 Enhanced SM (ESM)

ESM overcomes the SE limitation inherent in SM by transmitting information through the use of symbols constellation points [40], ESM transmits data using a variable combination of spatial indexing and symbol constellation points. For $N_{Tx} = 2$ and with APM of order M, the spectral efficiency of ESM for two antennas is given as,

$$\eta = \log_2 M + 2 \tag{2.45}$$

2.8.4 MRM

Since SM uses antenna index, i.e., spatial domain, to convey information, it demands that channel coefficients for the active antennas be sufficiently diverse; consequently, rich scattering is highly needed for better performance. Another challenge of classical SM is that transmit diversity is not achieved [35].

Consequently, the SM mentioned above and its variants; are likely to lose information if a similar channel exits in the environment. Although ESM can overcome this due to the use of power levels to detect antenna indices instead of the spatial domain, it requires additional transceiver design, hence hardware complexity.

Multiple Rank Modulation (MRM) introduced by [41], [42] , mitigates these challenges by cleverly using multiple antennas known as rank index as source of information, in each rank for a given time slot, the same information is transmitted hence all benefits of classical SM are enjoyed. MRM uses various channel shapes to decode the ranking index, and since a given rank has varying channels, the ranking index can be decoded even if the channels are alike [41]. Figure 2.16 [41] shows the MRM System model and Table 2.3 its Mapping table rule.

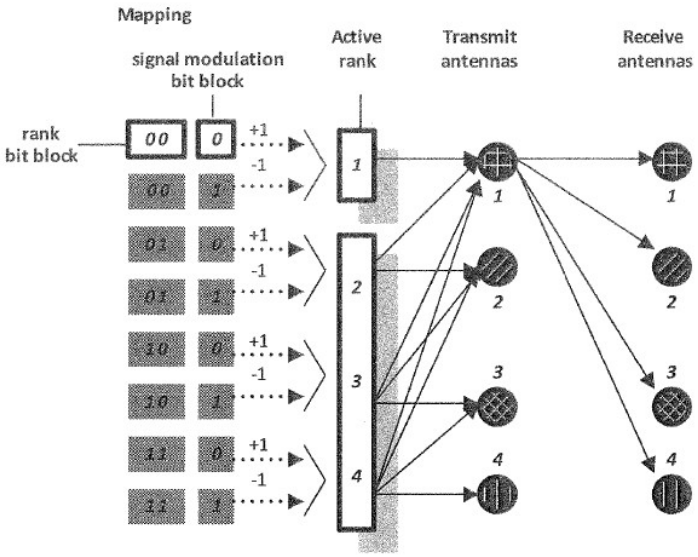

Figure 2.16: MRM System model

Table 2.3: MRM Mapping Table

	Example of MRM Mapping Rule		
Input bits b	**Antenna bits**	**Antenna index**	**BPSK Modulation bits**
000	00	1	+1
001	00	1	−1
010	01	1 , 2	+1
011	01	1 , 2	−1
100	10	1 , 2 , 3	+1
101	10	1 , 2 , 3	−1
110	11	1 , 2 , 3 , 4	+1
111	11	1 , 2 , 3 , 4	−1

2.8.5 Polar coded spatial modulation - PCSM

In the proposed work by [43], where the need to transmit index of antennas is eliminated by using polar codes, scheme termed as polar coded spatial modulation (PCSM). The proposed PCSM modulates the symbol bits using an M-ary quadrature amplitude modulation (MQAM) technique, whereas the bits that identify the transmit antenna index are a predetermined random sequence stored into the frozen polar set, and this sequence is likewise known at the receiver. As a result, the bits that identify the antenna index do not need to be transmitted to the receiver. The main contribution of this work was to eliminate the overheads of detec-

tion complexity. The work is unfortunately has limited applications since the requirement for $N_{RX} \geq N_{TX}$ is highly emphasized, also longer code block length with a lower code rate is required.

2.8.6 Layered Baud-Spatial Modulation

Scheme proposed by [44] where lower number of receive antennas are used than classical SM but with same data rates achieved and lower complexity was realized. LSM transmits the APM symbols via multiple asynchronous transmissions (MAT) within a single baud-space period and also makes use of the spatial domain to convey additional information to the receiver. In the design the received signal are over-sampled through fractional sampling (FS) and later combined before detection. Although FS may achieve multi-path diversity gains with limited number of receive antennas, multiple de-modulators are required for FS.

2.8.7 Subcarrier-Index Modulated OFDM (SIM-OFDM)

SIM-OFDM was introduced in [45], in which a portion of the sub-carriers are modulated by QAM and the indices of these activated sub carriers from each OFDM symbol or block are defined by the respective majority bit-values of an on-off-keying (OOK) stream of data. SIM-OFDM, on the other hand, has an unsteady data rate due to the random nature of the OOK data stream, which can lead to burst of errors.

2.8.8 Pulse Index Modulation (PIM)

In [46], the pulse index modulation (PIM) as well as generalized (G)PIM techniques are developed, wherein information is conveyed via Hermite-gaussian pulse shape and size rather than antenna indexing.

2.8.9 Sequence Modulation

Frequency sequence modulation (FSM) is a new transmission method which is based on a sequence of center carrier-frequencies to transmit data. [47] It is a variant of sequence modulation (SqM) system described in the patent [48]. The FSM is inspired by genetic-coding, in which three nucleotides represent up to twenty amino acids. The similarity enables building of less complex system that communicates using only three sub-carriers.

SqM also includes antenna-symbol (ASM) [49] and code-word (ACSM) [50] and symbol only (SSM) [51] in sequence modulation. In SqM schemes, the sequence patterns of transmit entities at the transmitter convey information. This thesis developed the use of wireless fading channels in unique sequence pattern to transmit information by mapping channel patterns of information bits onto SSK technique.

2.9 Knowledge Gap / Motivation

The aforementioned Spatial modulation techniques illustrate that the transmit antennas used impacts the spectral-efficiency of 'bits per channel use' - bpcu. Classical SM, GSM, ESM, MRM, and (G)PIM all use APM in addition to antenna indexing for conveying information. This means at the receiver side, two detection are needed, i.e., antenna index and APM symbol, which leads to transceiver detection complexity and power consumption than in SSK. SSK transmits information using only antenna indexing. This reduces detection complexity, but achievable data varies linearly with the number of antennas; 16 antennas are needed to transmit 4 bits.

CHAPTER THREE

PROPOSED SCHEME - SPACE SHIFT KEYING SEQUENCE MODULATION (SSK-SqM)

The SqM schemes reviewed in section 2.8 each uses an extra resource to convey information apart from the spatial domain, frequency, antenna code, and word code. The scheme developed here uses channels only to convey information, hence much less complexity than former variants of SqM. By cleverly using antenna patterns in the SSK technique and mapping three unique source channels to 4 bits. In comparison to classical SM and its variants, the new scheme can accommodate an odd number of transmit antennas, three, in a unique order for transmitting information, and able to achieve increased data rate than the conventional SSK, but lower than the other SM variant. In terms secrecy enhancement SSK-SqM outperformed the conventional SM and SSK, 4-QAM SIMO, and ASM, this is accomplished through the mapping of incoming sequences to a given sequence at the transmitter.

3.1 SSK-SqM System Model

Figure 3.1 depicts the SSK-SqM system concept, which consists wireless paths, with multiple antennas at receiver and transmitter, specifically three at transmitter and $3-5$ for receiver.

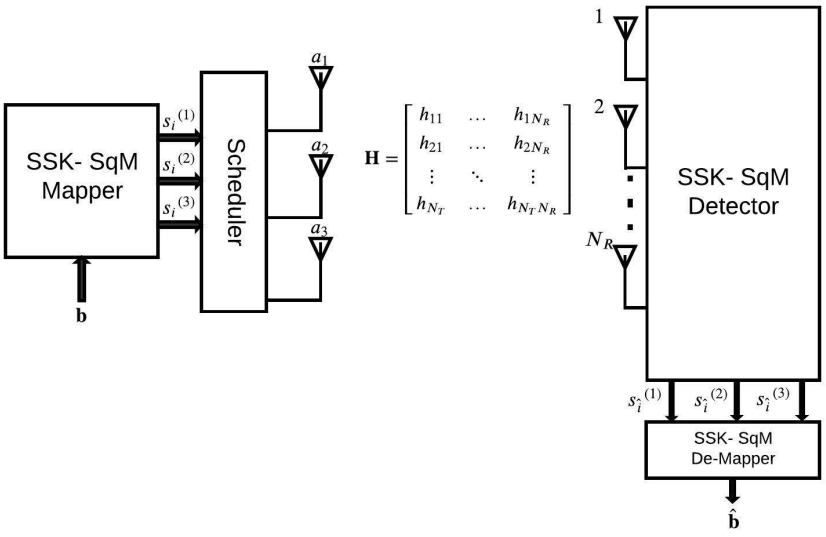

Figure 3.1: SSK-SqM System Model.

Incoming bits b are sent through the proposed model mapper, and segmented as, $m_b = \log_2 2^{N_t+1}$ bits and assigned to the vector associated with the known constellation,

$$s_i^{(j)} = \begin{bmatrix} s_i^{(1)} & s_i^{(2)} & s_i^{(3)} \end{bmatrix}^T \tag{3.1}$$

according to the mapper rule table described in Table 3.1 with power constraint of unity(i.e., $E_s\left[s^H s = 1\right]$). For SSK-SqM, in any given instant, just one antenna is engaged, during transmission, and therefore only one non-zero element entry of $s_i^{(j)}$'s in s. Signal is then sent through channel H and is influenced by AWGN $n = [n_1, n_2, \ldots, n_{Nr}]^T$. At the j-th time-slot, the received signal is as,

$$\mathbf{r}^{(j)} = \mathbf{H}\mathbf{s}_{ij}^{(j)} + \mathbf{n}^{(j)} \tag{3.2}$$

where $\mathbf{n}$ is iid entry as per $\mathbb{C} \sim \mathbb{N}(0, 1)$. Maximum Likelihood-detector at receiver, approximates channel mapping index $s_{\hat{i}}^{(j)} = \begin{bmatrix} s_{\hat{i}}^{(1)} & s_{\hat{i}}^{(2)} & s_{\hat{i}}^{(3)} \end{bmatrix}^T$ used in a given time-slot and de-maps the to estimated incoming bits $\hat{b}$, after all three estimates from time-slots are received. Table 3.1 illustrates mapper rule table of SSK-SqM, where s_i denotes the source channel from i (s_i). The three transmit antennas are set-up to convey information via sequence of pattern.

Table 3.1: SSK-SqM Mapper

Input bits b	**Tx Antenna Source Channels**		
	First TS $j = 1$	**Second TS** $j = 2$	**Third TS** $j = 3$
0000	s_1	s_1	s_1
0001	s_1	s_1	s_2
0010	s_1	s_1	s_3
0011	s_1	s_2	s_2
0100	s_1	s_2	s_3
0101	s_1	s_3	s_2
0110	s_2	s_2	s_2
0111	s_2	s_2	s_1
1000	s_2	s_2	s_3
1001	s_2	s_1	s_1
1010	s_2	s_3	s_1
1011	s_2	s_1	s_3
1100	s_3	s_3	s_3
1101	s_3	s_3	s_1
1110	s_3	s_3	s_2
1111	s_3	s_2	s_2

3.1.1 SSK-SqM Transmission

SSK-SqM is based on the idea of transmitting information using only channels in a pattern. A distinct pattern is employed to transmit messages as per the table 3.1. Thus, for the postulated SSK-SqM, we employ three antennas sequentially to convey four bits, because three time-slots are being utilized, then SE equals to 4/3 bits per channel use (bpcu), this is significant since the SE possible with three antennas in traditional SSK and SM is one.

As an illustration, let incoming bit b be [0000 0011 1010], then segmented to m groups, based on the mapper rule in Table 3.1. Segment 0000 is then assigned to $[s_1 \quad s_1 \quad s_1]$ and transmitted as s_1 in j^{th} Time-slot one, and again s_1 in $j = 2$ as depicted in Table 3.2, where i is i^{th} activated channel path in time-slot j^{th}. Therefore, s_{ij} implies N_j-dimensional vector, where N_j known, each constellation point symbol is conveyed through a given TS j, $j \in [1 : N_j]$, as an illustration, active antenna one in TS one is given as $s_{ij} = [s_{i1} \quad 0 \quad 0]^T$.The symbols s_{ij} in Table 3.2 are known, i.e., $\mathbf{s}_{ij} = s_{i1} = s_{i2} = s_{i3}$.

Table 3.2: SSK-SqM Transmission Example

$\mathbf{b}=[b_1 \quad b_2 \quad b_3 \quad b_4]$	**TS**	j	$\mathbf{s}_{ij} = [s_{i1} \quad s_{i2} \quad s_{i3}]^T$
[0 0 0 0]	1	1	$[1 \quad 0 \quad 0]^T$
	2	1	$[1 \quad 0 \quad 0]^T$
	3	1	$[1 \quad 0 \quad 0]^T$
[0 0 1 1]	1	1	$[1 \quad 0 \quad 0]^T$
	2	2	$[0 \quad 1 \quad 0]^T$
	3	2	$[0 \quad 1 \quad 0]^T$
[1 0 1 0]	1	2	$[0 \quad 1 \quad 0]^T$
	2	3	$[0 \quad 0 \quad 1]^T$
	3	1	$[1 \quad 0 \quad 0]^T$

3.1.2 SSK-SqM ML Detector

The ML-detector determines the active channel indexes for each TS assigned at transmitter. Considering that every active channel stream entries are equally probable, then ML-detector is thus represented as,

$$\mathbf{s}_{\hat{ij}}^{(j)} = \arg\max_{\mathbf{s_{ij}^{(j)}}} \; p_R\left(\mathbf{r}^{(j)}\middle|\mathbf{s}_{ij}^{(j)}, \mathbf{H}\right) \tag{3.3}$$

$$= \arg \; \min_{\mathbf{g}_{ij}^{(j)}} \left[\parallel \mathbf{g}_{ij}^{(j)} \parallel^2 -2\Re\left(\mathbf{r}^{(i)H}\mathbf{g}_{ij}^{(j)}\right)\right] \tag{3.4}$$

where $\mathbf{g}_{ij}^{(j)} = \mathbf{h}_j^{(j)} s_i$, $j \in [1 : N_j]$, , $i \in [1 : M]$, PDF of $\mathbf{r}$ given H & s_{ij} for a single SSK-SqM stream is written as,

$$p_R\left(\mathbf{r}^{(j)}\middle|\mathbf{s}_{ij}^{(j)}, \mathbf{H}\right) = \pi^{-Nr} \exp\left(-\parallel \mathbf{r}^{(j)} - \mathbf{H}\mathbf{s}_{ij}^{(j)}\parallel_F{}^2\right) \tag{3.5}$$

3.2 THEORETICAL FRAMEWORK

The SSK-SqM scheme's performance metric is deduced by utilizing method formulated by [25] for analysis of MA-SM system using single close-from BEP equation. Same techniques is applied intuitively to analyze SSK-SqM model. The technique employs error evaluation analysis of SIMO configuration to compute the BEP for typical SM schemes. A concept is applied in which an comparable equivalence bits in error is evaluated from the two criteria known as mutual information (MI) as well as sample variance (SV) and employed to determine the combined BEP for the spatial and modulation domains. The actual SEP with square M-ary M-QAM is given in [insert], typical SIMO system. Equivalent SEP,

$$P_{s-SIMO}\left(e|\bar{\gamma}\right) = aQ\left(\sqrt{b\bar{\gamma}}\right) - 4a^2Q^2\left(\sqrt{b\bar{\gamma}}\right) \tag{3.6}$$

where, $a = \left(1 - \frac{1}{\sqrt{M}}\right)$, $b = \left(\frac{3}{M-1}\right)$ and $Q\left(\bullet\right)$, $Q^2\left(\bullet\right)$, are Craig's first and second equations given as,

$$Q\left(\xi\right) = \frac{1}{\pi}\int_0^{\frac{\pi}{2}} \exp\left(-\frac{\xi^2}{2\sin^2\theta}\right)d\theta \tag{3.7}$$

and

$$Q^2\left(\xi\right) = \frac{1}{\pi}\int_0^{\frac{\pi}{4}} \exp\left(-\frac{\xi^2}{2\sin^2\theta}\right)d\theta. \tag{3.8}$$

$Q(\xi)$ and $Q^2(\xi)$ can be approximated using definite integral approximation-trapezoid rule,

$$\int_{\alpha}^{\beta} f(x)\,dx = \frac{\beta-\alpha}{N}\left[\frac{f(\alpha)+f(\beta)}{2} + \sum_{\kappa=1}^{N-1} f\left(\alpha+\kappa\frac{\beta-\alpha}{N}\right)\right] \tag{3.9}$$

as

$$Q(\xi) = \frac{1}{2N}\left[\frac{\exp\left(\frac{-\xi^2}{2}\right)}{2} + \sum_{\kappa=1}^{N-1}\exp\left(\frac{-\xi^2}{2sin^2\theta_k}\right)\right] \tag{3.10}$$

and $Q^2(\xi)$ as ,

$$Q^2(\xi) = \frac{1}{4M}\left[\frac{\exp(-\xi^2)}{2} + \sum_{\kappa=1}^{2M-1}\exp\left(-\frac{\xi^2}{2sin^2\beta_\kappa}\right)\right] \tag{3.11}$$

The SEP in 3.6 is simplified as,

$$P_{s-SIMO}(e|\bar{\gamma}) = \frac{a}{z}\left[\frac{1}{2}\exp(-\frac{b\bar{\gamma}}{2}) - \frac{a}{2}\exp(-b\bar{\gamma})\right] + \frac{a}{z}\left[(1-a)\sum_{i=1}^{z-1}\exp(-\frac{b\bar{\gamma}}{S_i}) + \sum_{i=z}^{2z-1}\exp(-\frac{b\bar{\gamma}}{S_i})\right] \tag{3.12}$$

z being the number of iterations and $S_i = 2\sin^2\left(\frac{\pi i}{4\lambda}\right)$. For fading channel, we average the P_{s-SIMO} over flat-fading distribution of the received SNR γ for the correlated channel. The average P_{s-SIMO} is then given as

$$E_\gamma\left[P_{s-SIMO}(e|\hat{\gamma})\right] = \int_0^\infty P_{s-SIMO}(e|\hat{\gamma})p_\gamma(\gamma)\,d\gamma \tag{3.13}$$

Evaluation of P_{s-SIMO} is even further modified through MGF [18],

$$\mathcal{M}_\gamma(s) = \int_0^\infty\cdots\int_0^\infty exp\left(-s\sum_{k=1}^{N_{Rx}}\gamma_k\right)\prod\left(p_\gamma(\gamma_k)\,d\gamma_k\right) = \prod\mathcal{M}_{\gamma_k}(s) \tag{3.14}$$

The transmitted SER denoted,Ps, is similar to M-QAM's average SER under diversity technique MRC over i.i.d Flat Fading channels in APM - MQAM. From [25], the SIMO SEP is given in its expanded version as the APM signal with ML detection, hence,

$$P_{s-SIMO} = \frac{a}{z}\left[\frac{1}{2}\prod_{k=1}^{N_{Rx}}\left(\frac{2}{b\bar{\gamma_\kappa}+2}\right) - \frac{a}{2}\prod_{\kappa=1}^{N_{Rx}}\left(\frac{1}{b\bar{\gamma_\kappa}+1}\right)\right] + \frac{a}{z}\left[(1-a)\sum_{i=1}^{z-1}\prod_{\kappa=1}^{N_{Rx}}\left(\frac{S_i}{b\bar{\gamma_\kappa}+S_i}\right) + \sum_{i=z}^{2z-1}\prod_{\kappa=1}^{N_{Rx}}\left(\frac{S_i}{b\bar{\gamma_\kappa}+S_i}\right)\right] \tag{3.15}$$

3.2.1 Joint-Antenna & Symbol BEP

Provided here, total SEP for SM scheme, P_{S-SM}, is available, then BEP,

$$P_B \leq \frac{P_{S-SM}}{b_{max}} \tag{3.16}$$

wherein *bmax* is indeed cumulative bits that can be transmitted via SM [6]. Hence, BEP of SM may be re-stated,

$$P_B = \frac{P_{S-SM}}{b_{max}} = \frac{P_{S-SIMO} v_e}{b_{max}} = \frac{P_{S-SIMO}}{b_e} \tag{3.17}$$

where v_e denotes the error-increasing coefficient above that of a SIMO space and $b_e = \frac{b_{max}}{v_e}$,is the corresponding SIMO system's bit error density. The challenge is to evaluate principal-components in combined space, which will be similar to b_e bits.

3.2.2 Effective error density in bits (b_e) for SSK-SqM

SSK-SqM model de-maps transmitted information after three time-slots are received. As a result, increased in detected errors with linear relationship transmit channel chains (N_a) over multiplexed space [25]. The fact that each covariance matrix element is formed in between 2 data,total covariance samples I_c in the concatenated space in ASM is calculated [25],

$$I_c = \binom{N_a}{2} = \frac{N_a!}{2!\,(N_a - 2)!} \tag{3.18}$$

For N_a chains over 3 times-lots, results in an increased of spatial-space N_{Tx} by factor I_c for every covariance chain stream, and this increase in space in turn reduces density bits by $I_c N_{Tx}$, as a result, the error is multiplied. Therefore, using the SV criterion, we can rewrite the channel and symbol bit density as,

$$b_{e,sv} = \frac{1}{I_c \sqrt{\frac{I_c N_{Tx}}{M\ -1}}} \tag{3.19}$$

Similarly, and in accordance with the MI criteria, we have, $q\,(x) = \frac{1}{I_c N_{tx}}$, whereas $p(x)$ is unchanged from $p\,(x) = \frac{1}{M-1}$ and consequently,

$$b_{e,MI} = \left| \log_2 \left(\frac{I_c N_{tx}}{M\ -1} \right) \right| \tag{3.20}$$

As an illustration, for $I_c = 1$ it conforms to SM. To optimally choose criteria to apply, lowest b_e is chosen,

$$b_{\mathrm{e,\ ASM}} = \min(b_{\mathrm{e,sv}}, b_{\mathrm{e,MI}}) \tag{3.21}$$

3.2.3 Overall Bit Error Rate for SSK-SqM

Equation 3.21 in conjunction with 3.17 and 3.18 can then be used to compute BEP of SSK-SqM as a factor of SER, P_{S-SM}, and b_e,as lower-bound average error. The average approximated PEB is then given as,

$$P_B = \frac{P_{S-SIMO}}{b_e(ASM)} = P_{ASM} \tag{3.22}$$

In estimating the SSK-SqM error, the contribution of SER error of conventional MQAM is removed from the joint-channel error. For 4QAM signal under SSK-SqM, the error for SSK-SqM joint channel and symbol error less BER of 4-QAM,

$$P_{SSK-SqM} \;=\; \left[\frac{P^{4QAM}_{S-SIMO}}{b_e\,(ASM)} \;-\; \frac{\eta_e P^{4QAM}_{S-SIMO}}{\log_2 M}\right] \tag{3.23}$$

where $\eta_e = 8$, combination of unique error source in patterns, for three time-slots (2^3). For SSK-SqM, $N_a = 3$, $I_c = 3$, $N_j = 3$, $M = 4$ and $\eta_e = 8$, are utilized to evaluate BEP of SSK-SqM. Equation 3.23 was used to find the probability error of the system developed.

3.3 Computational Complexity

Main benefit of SM systems is lower receiver complexity due to simpler receiver architecture design, compared to SMX and other MIMO systems. Further, SSK based systems have reduced complexity compared to classical SM systems. The receiver's computational complexity is measured by counting the quantity of arithmetical operations, i.e., real multiplication / division operations. For two complex multiplication four real multiplication are performed [1]. Considering Equation 3.5, for N_{Rx},is expressed,

$$\sum_{k=1}^{N_{Rx}} |\mathbf{r}(k)^{(j)} - \mathbf{H}(k)\mathbf{s}_{ij}^{(j)}(k)|^2 \tag{3.24}$$

For SM based systems $\mathbf{s}_{ij}^{(j)}$ is unknown, hence computational of $\mathbf{H}(k)\mathbf{s}_{ij}^{(j)}(k)$ will require four real multiplication and extra four for the square, resulting eight operations, performed over N_{Rx} times over cardinality of the input bits set , $2^{\eta_{SE}}$, where η_{SE} is the spectral efficiency for the given SM scheme. Therefore computational complexity of SM- based scheme is given as,

$$\mathcal{O}(SM) = 8N_{Rx} \times 2^{\eta_{SE}} \tag{3.25}$$

[1] $(x + jy)(n + jm) = (x \times n - y \times m) + j(x \times m + y \times n)$

For SSK-SqM scheme, $\mathbf{s}_{ij}$ is known, hence only square operation is needed, following same argument as that of SM-based system, we derived receiver computational complexity for SSK-SqM as,

$$\mathcal{O}(SSK - SqM) = 4N_{Rx} \times 2^{\eta_{SSK-SqM}} \tag{3.26}$$

3.4 Secrecy Rate - SSK-SqM

The performance of SSK-SqM can be compared to that of conventional SIMO systems, particularly in terms of physical layer security. As a result, because data is transmitted across three time slots, SSK-SqM is evaluated for secrecy rate. The secrecy rate is known to be difference in mutual information between legitimate user and eves dropper, normally termed as Bob and Eve respectively. Using MIMOME wiretap model [52] where legitimate and eavesdropper matrix channel are presented as $\mathbf{H}_b$ and $\mathbf{H}_e$ respectively, hence the received signal for Bob and Eve is given as,

$$\mathbf{y}_b = \mathbf{H}_b\mathbf{s} + \mathbf{n}_{y_b} \tag{3.27}$$

$$\mathbf{y}_e = \mathbf{H}_e\mathbf{s} + \mathbf{n}_{y_e} \tag{3.28}$$

For $N_{RX_e} \leq N_{RX_b}$, the MIMOME secrecy capacity for SSK-SqM can be evaluated as,

$$C_{SSK-SqM} = \max_{\mathbf{P}_S(s)}(I(\mathbf{s};\mathbf{y}_b|\mathbf{H}_b) - I(\mathbf{s};\mathbf{y}_e|\mathbf{H}_e)) \tag{3.29}$$

and achievable secrecy rate as,

$$R_s^{SSK-SqM} = \max\{0, I(\mathbf{s};\mathbf{y}_b|\mathbf{H}_b) - I(\mathbf{s};\mathbf{y}_e|\mathbf{H}_e)\} \tag{3.30}$$

Mutual information for MIMO system can shown to be [53],

$$\begin{aligned} I(\mathbf{s};\mathbf{y}|\mathbf{H}_e) = \mathtt{E}_{\mathbf{H}}\Bigg\{ \sum_{x\in\mathbf{S}} \int_y P_{\mathbf{SY}|\mathbf{H}}(s,y|\mathbf{H}) \times \\ \log \frac{P_{\mathbf{SY}|\mathbf{H}}(s,y|\mathbf{H})}{P_{\mathbf{S}|\mathbf{H}}(s|\mathbf{H}) P_{\mathbf{Y}|\mathbf{H}}(y|\mathbf{H})} dy \Bigg\} \end{aligned} \tag{3.31}$$

Equation 3.31 can be expressed in terms of entropy $\mathtt{H}_E(\mathbf{y}|\mathbf{s}_m, H)$ as,

$$\begin{aligned} I(\mathbf{s};\mathbf{y}|H) &= \mathtt{H}_E(\mathbf{y}, H) - \mathtt{E}_\theta\left[\mathtt{H}_E(\mathbf{y}|\mathbf{s}_m, H)\right] \\ &= \beta + \mathtt{E}_\theta\left[\mathtt{H}_E(\mathbf{y}|\mathbf{s}_m, H)\right] \\ \mathtt{H}_E(\mathbf{y}|\mathbf{s}_m, H) &= \sum_{x_m\in M} p(\mathbf{y}|\mathbf{s}_m, H)\log_2 p(\mathbf{y}|\mathbf{s}_m, H) \end{aligned} \tag{3.32}$$

From Fano's inequality,

$$\mathtt{H}_E(S|Y) \leq \mathtt{H}(e) + P(e)\log_2(|\chi|) \tag{3.33}$$

the inequality can be strengthened by replacing $|\chi|$ with $|\chi| - 1$ the equivocation, $\mathtt{E}_\theta\left[\mathtt{H}_E(S|Y)\right]$ is given by

$$\mathtt{H}_E(S|Y) \leq \mathtt{H}(e) + P(e)\log_2(|\chi| - 1) \tag{3.34}$$

where $\mathtt{H}(e)$, is given by,

$$\mathtt{H}(e) = P(e)\log_2 P(e) - [1 - P(e)]\log_2[1 - P(e)] \tag{3.35}$$

Using Equation 3.23 in Equation 3.34, then Equation 3.32 is solved, and hence achievable secrecy rate (Eq.3.30) is evaluated for given SNR.

CHAPTER FOUR

RESULTS AND DISCUSSION

4.1 BER Performance

To illustrate performance metrics of the suggested technique, BER, computational complexity and secrecy rate for SSK-SqM is examined. The traditional SSK is utilized as a benchmark. The SNR used in monte-carlo numerical simulations is $\frac{E_s}{N_0}$, whereas E_s and N_0 are energy per

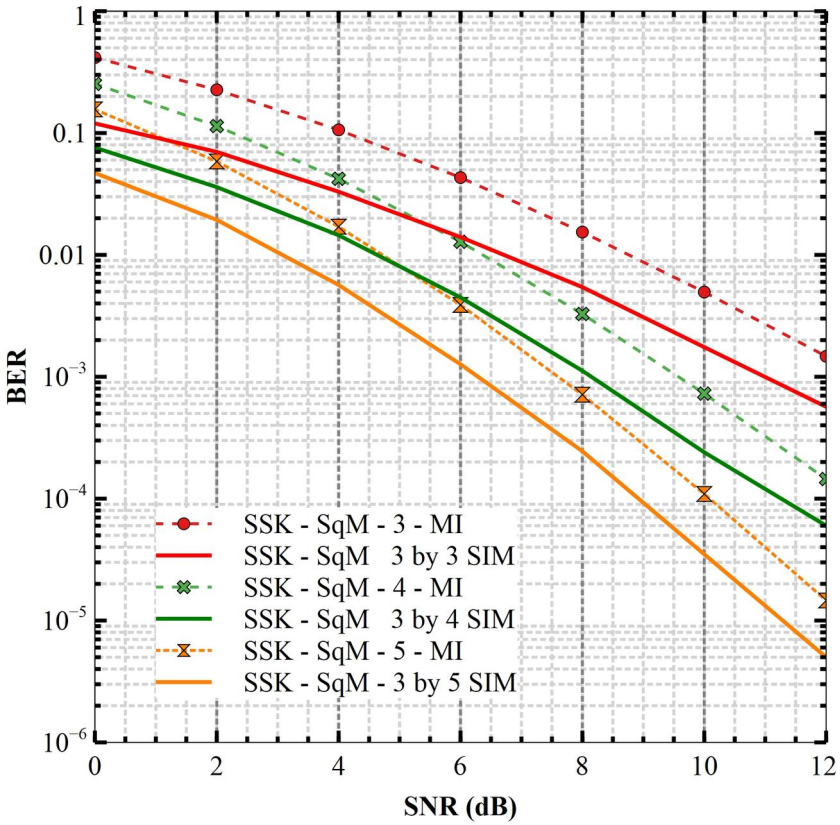

Figure 4.1: BER of SSK-SqM with Nr = 3, 4, 5 - MI Criteria

symbol and noise respectively. Maximum Likelihood detection is considered at the receiver. Transmit entity are Flat Fading channels, i.e., Rayleigh/Racian.

Figure 4.1 illustrates the theoretical and Numerical simulation performance plots of SSK-SqM with Nr = 3, 4, 5 for MI criteria. The channel considered is Rayleigh Flat fading in the pattern sequences. In Figure 4.1 simulations deviates from MI criteria, this is beacuse MI criteria uses

probabilistic distance between symbols to determine error probability among symbols and since our proposed scheme solely uses sequence of Gaussian channel to convey information, hence deviation. In the case of the SV criteria, as shown by the Figure 4.2, both analytical and

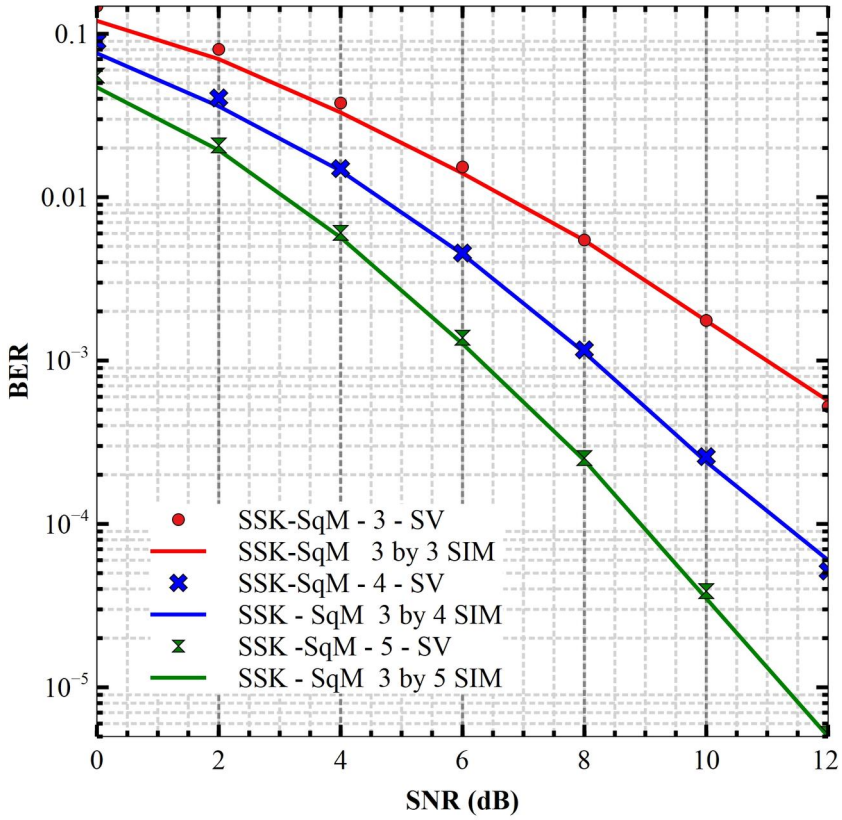

Figure 4.2: SSK-SqM Performance at 4/3 SE with $N_{RX} = 3$ to 5 - SV

simulation outputs concur well over the SNR range.

Furthermore, Figure 4.3 depicts BER of SSK-SqM with four receive antennas compared with SSK. At 10^{-4}BER, the proposed model needs 1dB additional power compared to classical SSK, although the proposed scheme can achieve extra a third bpcu for 3 by 4 SSK.

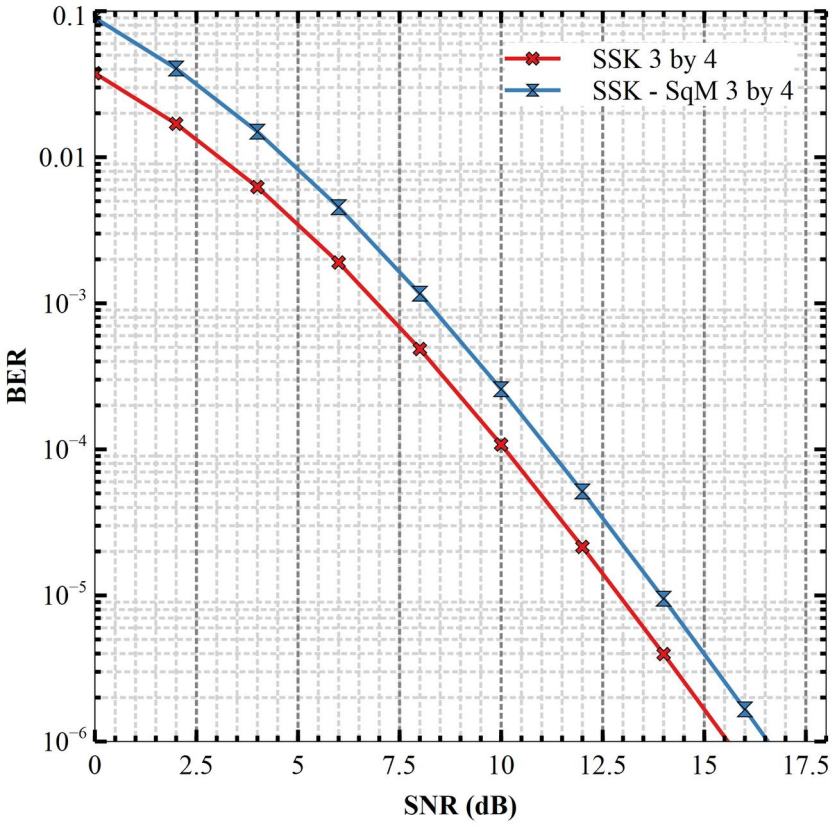

Figure 4.3: Performance Compar1son of SSK vs. SSK-SqM, $N_{RX} = 4$.

Further simulations were performed as illustrated in Figure 4.4, in demonstrating SSK-SqM performances under the Rayleigh vs. Racian channel. It is noticed that for the same BER of 10^{-4} Racian channel required an extra of 7.5 dB than that of Rayleigh channel. Hence, the poor Rayleigh channel was observed to behave better than the good Racian channel. It is because

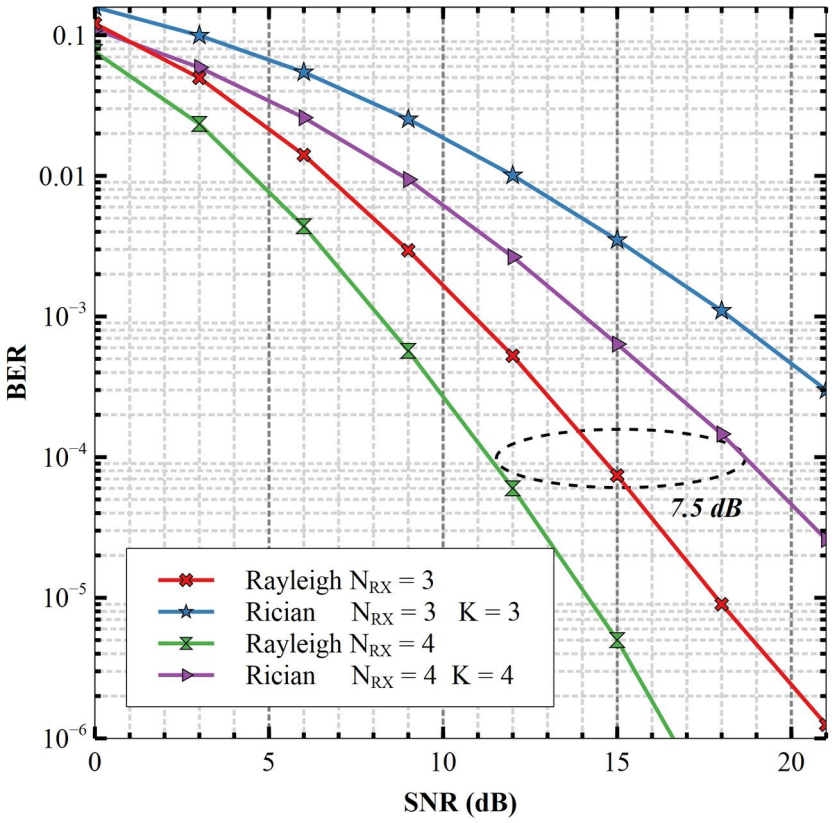

Figure 4.4: SSK-SqM under Rayleigh/Rician Channels.

channels are exclusively utilized to transfer information, therefore there is less error detection towards a more dispersed channel than a less scattering channel.

Figure 4.5 shows simulations under correlated Rayleigh and Rician channel with Rice factor $K = 10$ and antenna spacing $d = 0.5\lambda$, where λ is the wavelength of the carrier. Simulations confirmed the previous results of uncorrelated channels showing rayleigh channel performing better. An extra 1 dB is needed for the same BER (10^{-3}). Correlated channel performance curve for antenna spacing $d = 0.1\lambda$ is depicted in Figure 4.6. Comparing Figure 4.5 and 4.6, it

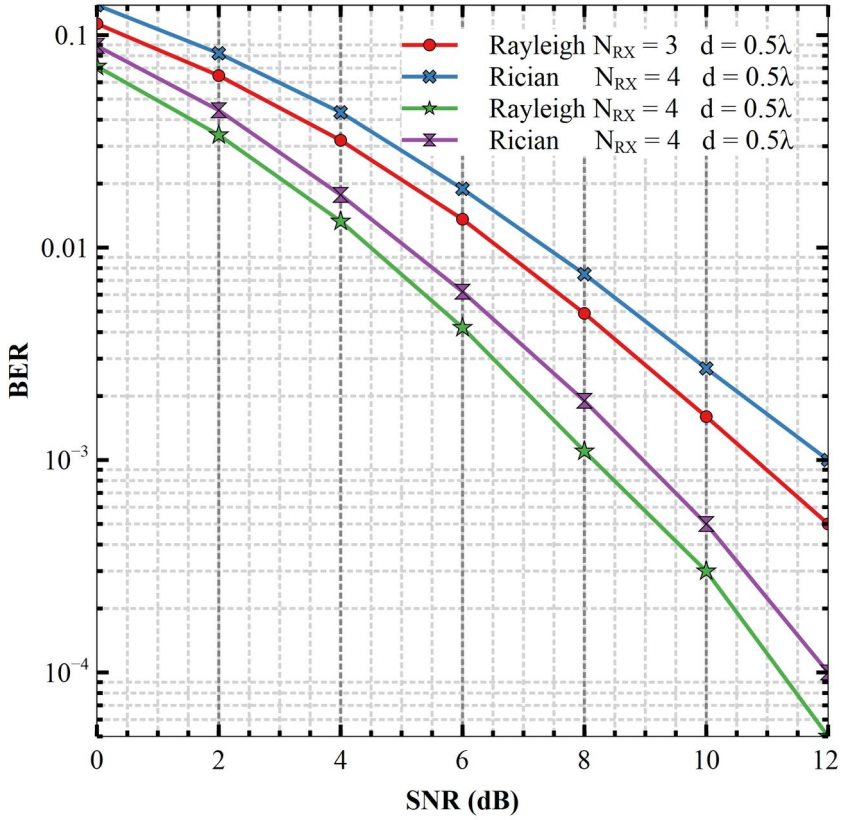

Figure 4.5: SSK-SqM under Correlated ($d = 0.5\lambda$) Rayleigh and Rician Channels (K = 10).

is noticed that the performance (BER) decreases as the antenna spacing is reduced, for example rayleigh channel with ($d = 0.1\lambda$) required an extra 5 dB for the same BER than that of spacing ($d = 0.5\lambda$). Due to closer interaction between antennas for reduced spacing, more errors are detected.

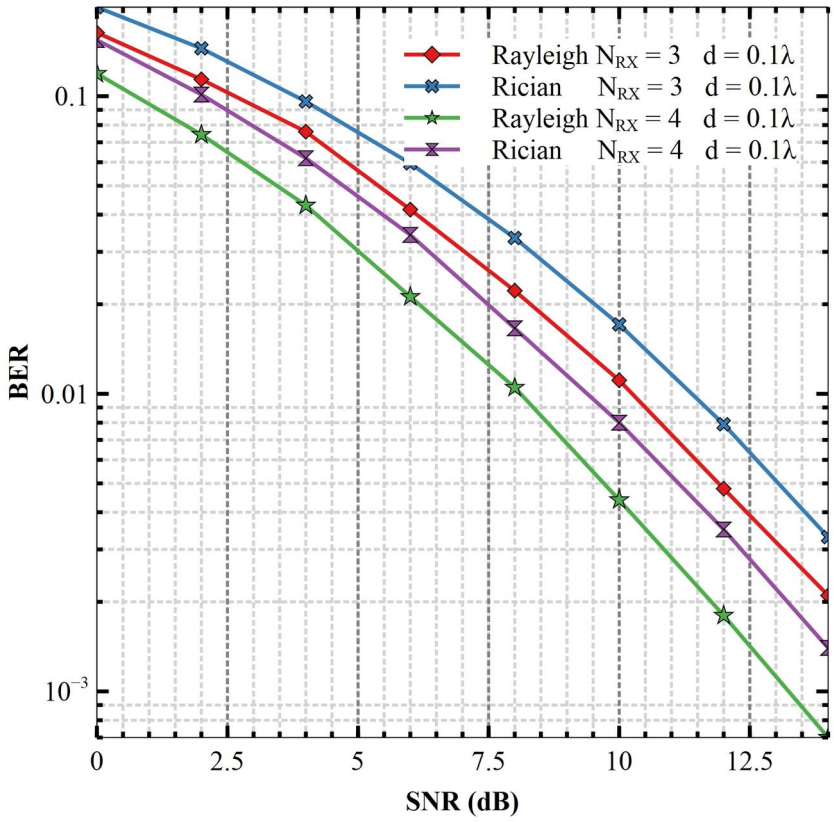

Figure 4.6: SSK-SqM under Correlated ($d = 0.1\lambda$) Rayleigh and Rician Channels (K = 10).

Additional comparisons with 4-QAM, SM, and ASM were made for completeness. As illustrated in Figure 4.7 and 4.8, the proposed model outperforms the aforementioned techniques in terms of BER performance. It is also noted that for the same BER of 0.01, SSK-SqM needs 6.5dB, while ASM(4-QAM) and ASM(BPSK) requires an extra 1 and 1.75 dB respectively.

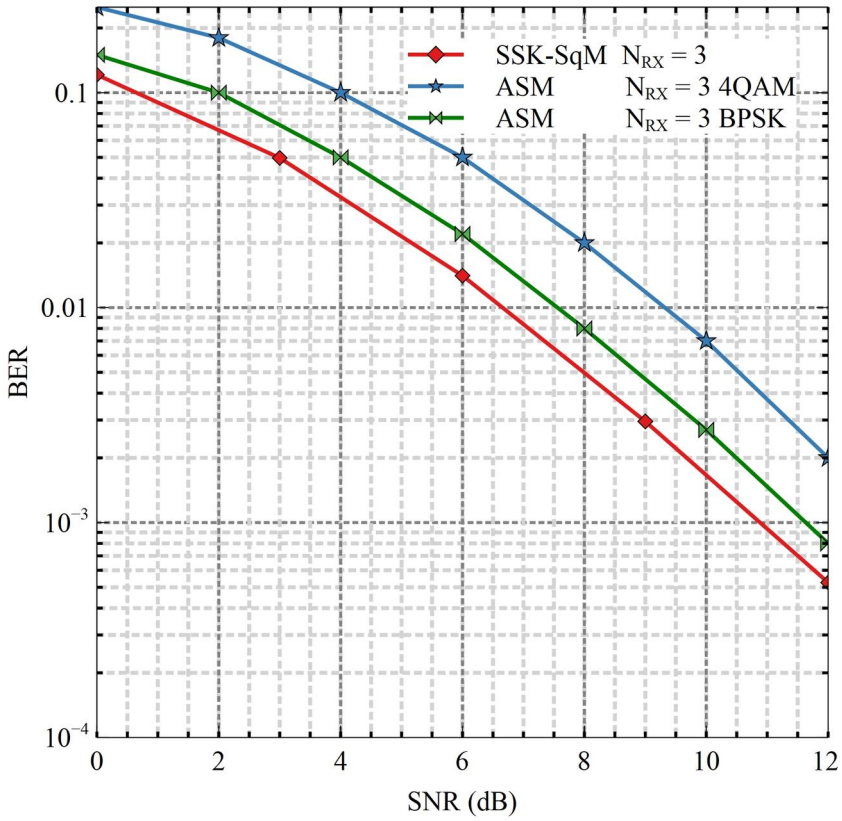

Figure 4.7: SSK-SqM vs. ASM (4QAM and BPSK)

In Figure 4.8, SSK-SqM achieved BER of 10^{-4} at SNR of 11.5 dB, whilst SM and 4-QAM SIMO at 12 and 13 dB respectively, this indicates performance superiority of SSK-SqM. More power is needed to attain for SM and SIMO-4QAM for the same performance.

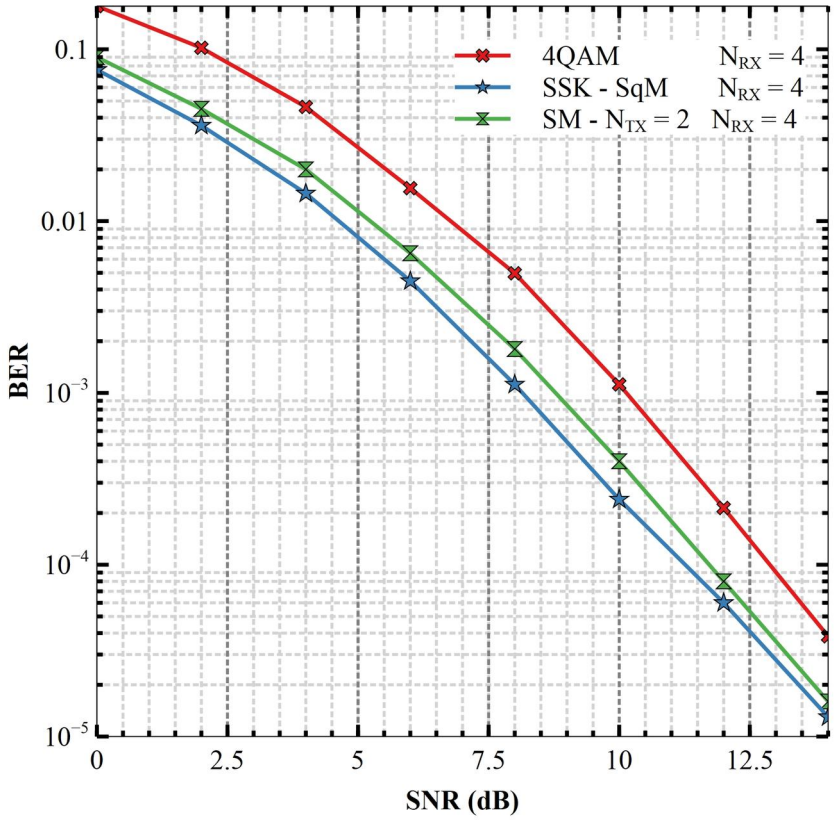

Figure 4.8: SSK-SqM vs. SM ($N_{TX} = 2, N_{RX} = 4$), 4QAM ($N_{RX} = 4$)

4.2 Receiver Computational Complexity

Computational complexity at receiver is analyzed From Equation 3.25 and 3.26. It is clear that using SSK-SqM complexity is lowered by 50% compared to classical SM, for the same SE, i.e, $\eta_{SSK-SqM} = \eta_{SM}$. Further for SE of $2bpcu$, the SM (with BPSK as APM) and classical SSK, the computational complexity at receiver of SSK-SqM is reduced by 40% and 62% when compared to SM and SSK respectively. This is illustrated in Table 4.1.

Table 4.1: Receiver Computational Complexity

Spectral Efficiency (SE)	SSK-SqM vs. SM	SSK-SqM vs. SSK	SSK vs. SM
1	–	126%	–
2	31%	62%	50%

4.3 Secrecy Rate

Secrecy rate was also analyzed for the proposed model and compared with Classical SM and SSK. Fig. 4.9 depicts the secrecy rate for the case with three receive antenna at the legitimate receiver and the eavesdropper.

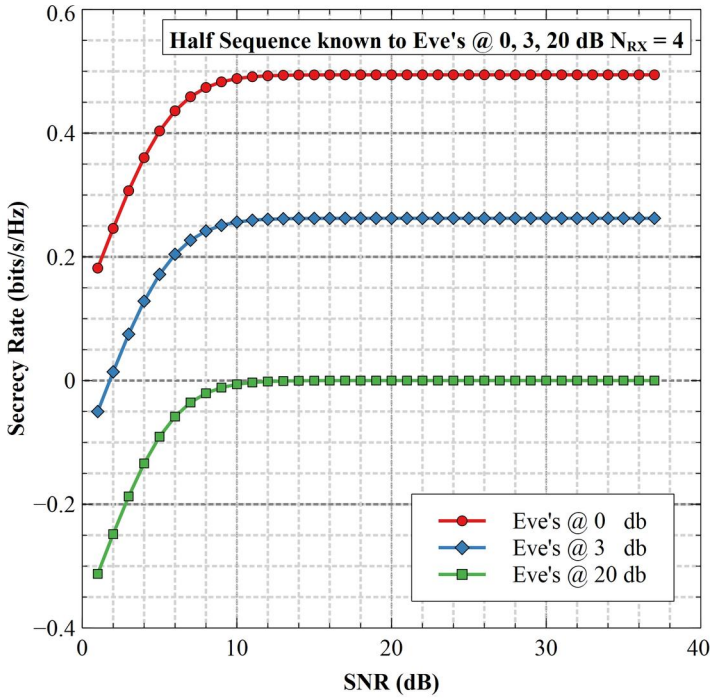

Figure 4.9: SSK-SqM Secrecy Rate with half sequence known to Eve.

This rate is evaluated by equation 3.30. In this analysis, we consider i.i.d. channel coefficients from N_{RX} antenna, the secrecy rate is averaged over many channel realizations and plotted versus Bob's signal SNR, while keeping Eve's SNR fixed at 0, 8 and 20 dB. This shows that more SNR given to eavesdropper the secrecy rate is lowered and vice-versa.

In Figure 4.10,secrecy capacity was evaluated by varying the legitimate receiver's SNR for three cases in which the eavesdropper's SNR was fixed at 0, 3, and 20 dB, respectively and compared with increasing number of receive antennas. Figure 4.10 shows that secrecy rate

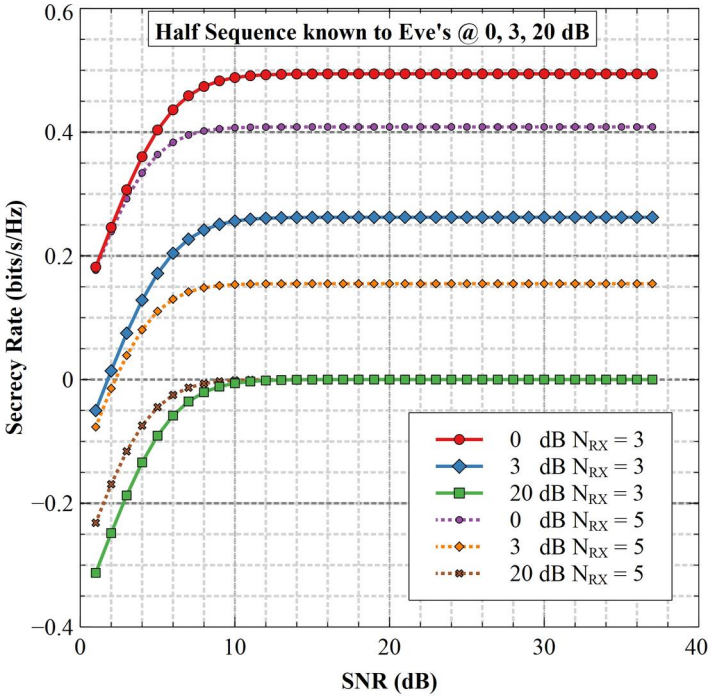

Figure 4.10: SSK-SqM Secrecy Rate, $N_{RX} = 3, 5$

is lowered when there is an increase in Eve's SNR, this is because increasing Eve's SNR we are actually reducing the SNR gap between Bob and Eve's, consequently reduced difference in mutual information. It is also noted that increasing the number of antennas at the legitimate receiver and the eavesdropper reduces the level of secrecy, this is due to the fact that capacity gain is achieved for both Bob and Eve, reduced mutual information between them.

Further comparisons of the SSK-SqM model's secrecy rate were conducted, as illustrated in Figures 4.11 and 4.12. The secrecy rate of SSK-SqM was compared to that of SIMO in Figure

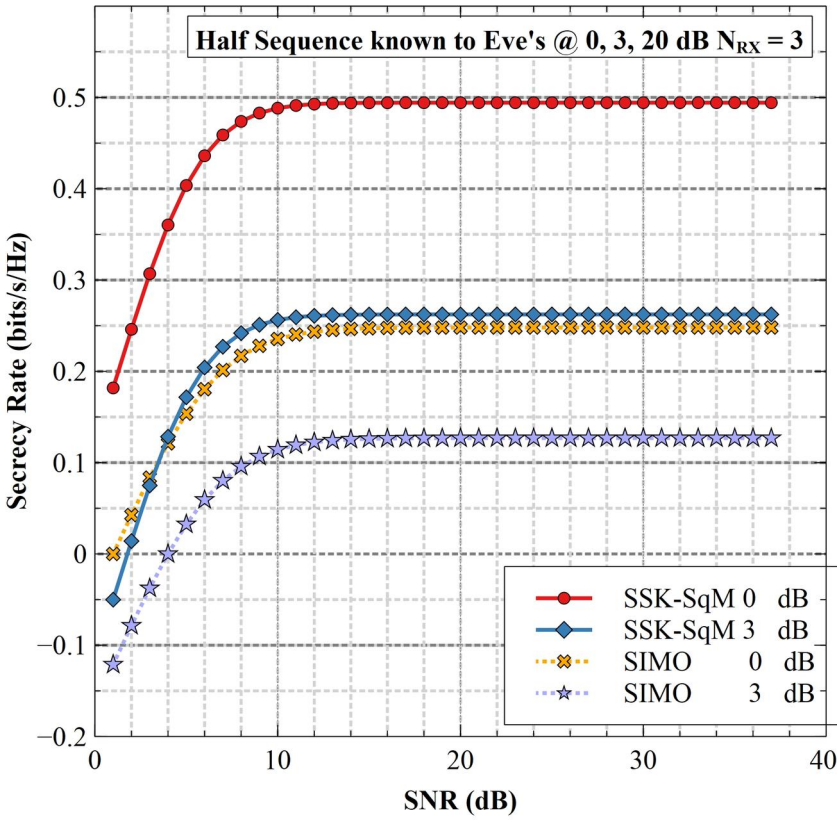

Figure 4.11: Secrecy Rate comparison: SSK-SqM vs 4QAM-SIMO.

4.11 and to that of SSK in Figure 4.12. SSK-SqM outperformed the SIMO and classical SSK in both cases and for the given Eve's scenario. This was due to the mapping table's design, since the mapper is only known to transmitter and legitimate user. Secrecy analysis was analyzed for the case when eavesdropper knows half of the mapper table. In this case low capacity is achieved compared to SSK-SqM (full mapper is known), and this turns to have high mutual information in the case SSK-SqM than SIMO, between Bob and Eve.

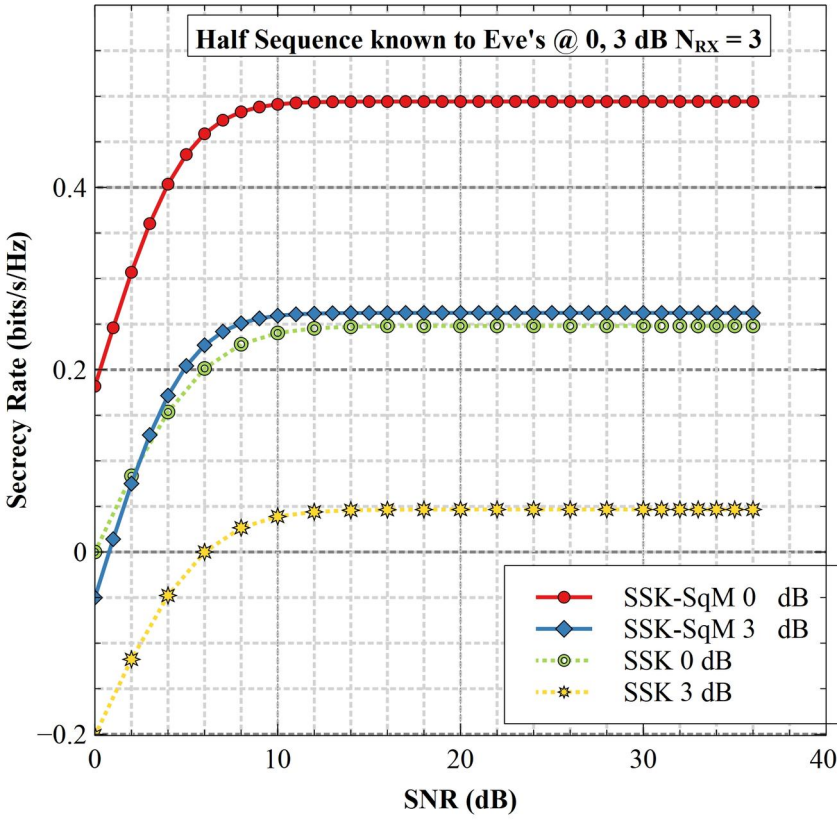

Figure 4.12: Secrecy Rate comparison: SSK-SqM vs SSK.

CHAPTER FIVE

CONCLUSION AND RECOMMENDATION

This thesis focused mainly on developing and analyzing SSK-SqM transmission technique for wireless communication systems operating on frequency-flat channels. This thesis's primary contributions and findings are summarized here.

5.1 Contributions and Findings

i) In section 3.1, a new transmission technique for a MIMO configuration was developed by combining SM-SSK and SqM (SSK-SqM) as depicted in the system model in Figure 3.1. The mapper rule for implementation of the system model was tabulated as in table 3.1,Which demonstrated how three transmit antennas are mapped in a predefined sequence set at the transmitter.

ii) The performance closed-form equation 3.23 developed was accurately validated with the Monte-Carlo simulations.

iii) The analysis of computational complexity at receiver of the proposed model is shown to be much less that the classical SSK and SM, a reduction of 40% and 62% respectively. This was due to the sequencing nature of the predefined mapping table in conveying information.

iv) The use of predefined mapping table in sequence to convey information also managed to enhance secrecy rate. The secrecy enhancement is shown in Figure 4.11 and 4.12, SSK-SqM achieved a secrecy rate of 0.5 bits/s/Hz while that of SIMO (4QAM) and conventional SSK is 0.25 bits/s/Hz and 0.22 bits/s/Hz respectively.

5.2 Conclusion

The novel SSK-SqM based scheme, which exploits both antenna indices and pattern in conveying information, accommodates the odd number of the antenna in transmission and additional SE of 1.333 bpcu than that of classical SSK.

The flat-fading channels used in conveying information showed that bad channel Rayleigh performed better than the Rician channel; this means that the proposed model can work in

a high scattering environment which is advantageous compared to other systems. Due to the uniqueness of the antenna pattern, this scheme was able to enhance security.

5.3 Recommendation

Secrecy enhancement achieved makes the scheme suitable for security sensitive scenario such as military, space communication. Future studies can be carried out to generalize the SSK-SqM for different set of transmit antennas, and using generalized fading distributions such as Nakagami-m, $\eta - \mu$, $\kappa - \mu$, and $\alpha - \mu$ fading as transmit entities.

REFERENCES

[1] Vincent WS Wong, Robert Schober, Derrick Wing Kwan Ng, and Li-Chun Wang. *Key technologies for 5G wireless systems*. Cambridge university press, 2017.

[2] David Tse and Pramod Viswanath. *Fundamentals of wireless communication*. Cambridge university press, 2005.

[3] Andrea Goldsmith. *Wireless communications*. Cambridge university press, 2005.

[4] Georgios B Giannakis, Zhiqiang Liu, Xiaoli Ma, and Sheng Zhou. *Space-time coding for broadband wireless communications*. John Wiley & Sons, 2007.

[5] Read Mesleh, Harald Haas, Chang Wook Ahn, and Sangboh Yun. Spatial modulation-a new low complexity spectral efficiency enhancing technique. In *2006 First International Conference on Communications and Networking in China*, pages 1–5. IEEE, 2006.

[6] Raed Y Mesleh, Harald Haas, Sinan Sinanovic, Chang Wook Ahn, and Sangboh Yun. Spatial modulation. 57(4):2228–2241, 2008. Publisher: IEEE.

[7] Antonis Kalis, Athanasios G Kanatas, and Constantinos B Papadias. A novel approach to MIMO transmission using a single RF front end. 26(6):972–980, 2008. Publisher: IEEE.

[8] Athanasios Stavridis, Sinan Sinanovic, Marco Di Renzo, Harald Haas, and Peter Grant. An energy saving base station employing spatial modulation. In *2012 IEEE 17th International Workshop on Computer Aided Modeling and Design of Communication Links and Networks (CAMAD)*, pages 231–235. IEEE, 2012.

[9] Geoffrey Ye Li, Zhikun Xu, Cong Xiong, Chenyang Yang, Shunqing Zhang, Yan Chen, and Shugong Xu. Energy-efficient wireless communications: tutorial, survey, and open issues. 18(6):28–35, 2011. Publisher: IEEE.

[10] Marco Di Renzo and Harald Haas. On transmit diversity for spatial modulation MIMO: Impact of spatial constellation diagram and shaping filters at the transmitter. 62(6):2507–2531, 2013. Publisher: IEEE.

[11] Tianqi Mao, Qi Wang, Zhaocheng Wang, and Sheng Chen. Novel index modulation techniques: A survey. 21(1):315–348, 2018. Publisher: IEEE.

[12] Cisco Visual Networking Index. Global mobile data traffic forecast upyear, 2016–2021 white paper. 7:180, 2017.

[13] Omar Hiari, Raed Mesleh, and Abdullah Al-Khatib. A system simulation framework for modeling space modulation techniques. 14(1):1435–1446, 2019. Publisher: IEEE.

[14] Mathuranathan Viswanathan. Simulation of digital communication systems using matlab. 2013.

[15] Nilesh Kalani, Dipti Anant, and GR Kulkarni. Performance analysis of linear modulation techniques with different channel coding in LabVIEW®. In *2013 International conference on Circuits, Controls and Communications (CCUBE)*, pages 1–5. IEEE, 2013.

[16] Michel Chino, Héctor Miyashiro, and A Jorge Luis. Implementation of SNR estimation algorithms, using LabVIEW communications and GNU radio companion. In *2018 IEEE XXV International Conference on Electronics, Electrical Engineering and Computing (INTERCON)*, pages 1–4. IEEE, 2018.

[17] M Divya. Bit error rate performance of BPSK modulation and OFDM BPSK with rayleigh multipath channel international journal of engineering and advanced technology (IJEAT) ISSN: 2249–8958. 2013.

[18] Marvin K Simon and Mohamed-Slim Alouini. *Digital communication over fading channels*, volume 95. John Wiley & Sons, 2005.

[19] Fuqin Xiong. *Digital Modulation Techniques, (Artech House Telecommunications Library)*. Artech House, Inc., 2006.

[20] Brijesh Kumbhani and Rakhesh Singh Kshetrimayum. *MIMO wireless communications over generalized fading channels*. CRC Press, 2017.

[21] Yunxia Chen and Chintha Tellambura. Distribution functions of selection combiner output in equally correlated rayleigh, rician, and nakagami-m fading channels. 52(11):1948–1956, 2004. Publisher: IEEE.

[22] John G. Proakis and Masoud Salehi. *Digital communications*. McGraw-Hill., 2008.

[23] Theodore S Rappaport and others. *Wireless communications: principles and practice*, volume 2. prentice hall PTR New Jersey, 1996.

[24] S Rice. *Mathematical analysis of random noise. Bell System Technical Journals, 23–24 (reprinted in "Selected Papers on Noise and Stochastic Processes", ed. Wax, 1954)*. New York: Dover, 1945.

[25] Peter Odero Akuon and Hongjun Xu. Performance of multiple active-spatial modulation: information theoretic criteria over correlated rayleigh fading channels. 10(9):1071–1079, 2016. Publisher: IET.

[26] Roger A Horn and Charles R Johnson. *Matrix analysis*. Cambridge university press, 2012.

[27] Manish Mandloi, Arijit Datta, and Vimal Bhatia. Index modulation techniques for 5g and beyond wireless systems. In *5G and Beyond Wireless Systems*, pages 63–83. Springer, 2021.

[28] Siavash M Alamouti. A simple transmit diversity technique for wireless communications. 16(8):1451–1458, 1998. Publisher: IEEE.

[29] Vahid Tarokh, Hamid Jafarkhani, and A Robert Calderbank. Space-time block codes from orthogonal designs. 45(5):1456–1467, 1999. Publisher: IEEE.

[30] Athanasios Stavridis, Sinan Sinanovic, Marco Di Renzo, and Harald Haas. Energy evaluation of spatial modulation at a multi-antenna base station. In *2013 IEEE 78th Vehicular Technology Conference (VTC Fall)*, pages 1–5. IEEE, 2013.

[31] Dushyantha A Basnayaka, Marco Di Renzo, and Harald Haas. Massive but few active MIMO. 65(9):6861–6877, 2015. Publisher: IEEE.

[32] Yaping Cui and Xuming Fang. Performance analysis of massive spatial modulation MIMO in high-speed railway. 65(11):8925–8932, 2016. Publisher: IEEE.

[33] Jeyadeepan Jeganathan, Ali Ghrayeb, and Leszek Szczecinski. Spatial modulation: Optimal detection and performance analysis. 12(8):545–547, 2008. Publisher: IEEE.

[34] Nigel Reece Naidoo, HJ Xu, and T Al-Mumit Quazi. Spatial modulation: optimal detector asymptotic performance and multiple-stage detection. 5(10):1368–1376, 2011. Publisher: IET.

[35] Ertugrul Basar, Miaowen Wen, Raed Mesleh, Marco Di Renzo, Yue Xiao, and Harald Haas. Index modulation techniques for next-generation wireless networks. 5:16693–16746, 2017. Publisher: IEEE.

[36] Jeyadeepan Jeganathan, Ali Ghrayeb, Leszek Szczecinski, and Andres Ceron. Space shift keying modulation for MIMO channels. 8(7):3692–3703, 2009. Publisher: IEEE.

[37] Jeyadeepan Jeganathan, Ali Ghrayeb, and Leszek Szczecinski. Generalized space shift keying modulation for mimo channels. In *2008 IEEE 19th International Symposium on Personal, Indoor and Mobile Radio Communications*, pages 1–5, 2008.

[38] Abdelhamid Younis, Nikola Serafimovski, Raed Mesleh, and Harald Haas. Generalised spatial modulation. In *2010 conference record of the forty fourth Asilomar conference on signals, systems and computers*, pages 1498–1502. IEEE, 2010.

[39] Jintao Wang, Shuyun Jia, and Jian Song. Generalised spatial modulation system with multiple active transmit antennas and low complexity detection scheme. *IEEE Transactions on Wireless Communications*, 11(4):1605–1615, 2012.

[40] Chien-Chun Cheng, Hikmet Sari, Serdar Sezginer, and Yu T Su. Enhanced spatial modulation with multiple signal constellations. 63(6):2237–2248, 2015. Publisher: IEEE.

[41] Hongjun Xu and Peter Odero Akuon. A multiple rank modulation system. *US Patent App. 15/756,564*, 2018.

[42] Andrew Nyawade, Peter O Akuon, Hongjun Xu, and Vitalis Oduol Kalecha. Spatial MIMO rank modulation. In *2019 IEEE AFRICON*, pages 1–6. IEEE, 2019.

[43] Peter Akuon and Hongjun Xu. Polar coded spatial modulation. *IET Communications*, 8(9):1459–1466, 2014.

[44] Peter Akuon and Hongjun Xu. Layered baud-space modulation. In *SATNAC*. SATNAC 2015, 2015.

[45] Rami Abu-Alhiga and Harald Haas. Subcarrier-index modulation ofdm. In *2009 IEEE 20th International Symposium on Personal, Indoor and Mobile Radio Communications*, pages 177–181. IEEE, 2009.

[46] Sultan Aldirmaz-Colak, Erdogan Aydin, Yasin Celik, Yusuf Acar, and Ertugrul Basar. Pulse index modulation. *IEEE Communications Letters*, 2021.

[47] Peter O Akuon. Frequency sequence modulation: Analysis of additional spectrum space. In *2019 IEEE AFRICON*, pages 1–4. IEEE, 2019.

[48] Peter Odero Akuon and Andrew Mwangi Kimani. Systems and methods for communication. *US Patent 11,258,491*, February 2022.

[49] Joseph Abok Obadha, Peter O Akuon, and Vitalis Oduol Kalecha. Ber performance of antenna sequence modulation (asm). In *2021 IEEE AFRICON*, pages 1–6. IEEE, 2021.

[50] Joseph Abok Obadha, Peter O. Akuon, and Vitalis Oduol Kalecha. Ber of antenna code sequence modulation (acsm) and analysis under repetition. In *2019 IEEE AFRICON*, pages 1–5, 2019.

[51] Peter O. Akuon. Ber analysis of symbol sequence modulation under non-fading awgn channels. In *2021 IEEE AFRICON*, pages 1–4, 2021.

[52] Sina Rezaei Aghdam, Tolga M Duman, and Marco Di Renzo. On secrecy rate analysis of spatial modulation and space shift keying. In *2015 IEEE International Black Sea Conference on Communications and Networking (BlackSeaCom)*, pages 63–67. IEEE, 2015.

[53] Thomas M Cover and Joy A Thomas. *Elements of Information Theory*. John Wiley & Sons, 2012.

APPENDIX A: PUBLICATIONS

IEEE AFRICON 2021

BER Performance of SSK Sequence Modulation

1st Abdulrahman A. Faris
Department of Electrical and Information Engineering
University of Nairobi
Nairobi, Kenya
abdulrahman.faris@gmail.com

2nd Peter O. Akuon
Department of Electrical and Information Engineering
University of Nairobi
Nairobi, Kenya
akuonp@yahoo.com

3rd Vitalis Oduol Kalecha
Department of Electrical and Information Engineering
University of Nairobi
Nairobi, Kenya
vitalice.oduol@gmail.com

Abstract—Space shift keying antenna sequence modulation (SSK-ASM) is proposed for conveying information bits through unique antenna sequence patterns. The information is conveyed in spatial domain only via mixed Gaussian channel such Rayleigh Flat Fading. In this paper we, present analytical formulation of bit error rate performance of SSK-ASM, by utilizing Sample variance (SV) and Mutual information (MI) criterion in single input Multiple output (SIMO) configuration. Moreover, the exact Average bit error probability (ABEP) over Rayleigh Flat fading channel is developed in close-form. Monte Carlo simulations is shown to be tightly bound to the theoretical framework for SV criterion method.

Index Terms—ABEP, Antenna Sequence Modulation, BER, Rayleigh Fading, SSK

I. Introduction

Multi-antenna system in wireless communication such as the vertical-Bell Laboratories Layered Space Time (V-BLAST) architecture allows spectral and data rate improvement over single antenna communication systems [1]. High spectral efficiency is achieved by utilizing transmission schemes designed for multiple input multiple output (MIMO)systems, such as V-BLAST. However, the technique suffer greatly inter channel interference (ICI) , inter antenna synchronization (IAS)and has high maximum likelihood (ML) detection complexity.Hence, designing systems which are capable of avoiding ICI and IAS can greatly reduce transceiver complexity, and in turn achieving performance improvements. [2]

In 2008, [3] proposed a novel way of conveying information bits, termed as spatial modulation (SM) to alleviate the aforementioned challenges of MIMO systems. SM has dominated research field in transmission techniques for the past two decades, which several SM variants were proposed. In Classical SM, single antenna is activated from the transmit antennas for transmission at one time instant. Incoming information bits are split into antenna index bits, and mapped to the active antenna indices, and modulated bits, which constitute constellation symbols. Hence, additional information is conveyed by active antenna indices among the constellation symbols. By using only one active antenna at one time instant, IAI and IAS requirement are evaded. The spectral efficiency of SM in terms of bits per channel use (bpcu) is given by,

$$\lfloor \log_2(N_t) \rfloor + \log_2(M) \tag{1}$$

where N_t and M denote number of transmit antenna and size of signal constellation diagram under consideration such as M-PSK or M-QAM.

A. Related Works

From equation 1 it is clear that the bpcu increases logarithmic-ally hence will require more antennas than in spatial multiplexing (SMX) MIMO system for the same data rate. SSK proposed in [4] is the simplest form of the family of Spatial Modulation Techniques (SMTs) even though it was proposed after SM, where spatial domain alone is used to convey information, hence greatly reduce tranceiver design complexity but at the expense of data rate reduction. Among the drawbacks of classical SM is that its spectral efficiency is proportional to logarithm of number of transmit antenna, and number of antennas need to be power of two, while SMX-MIMO spectral efficiency increases linearly with N_t, which means that SM will need more transmit antennas than SMX-MIMO for the same spectral efficiency. These challenges were overcome by introduction of generalized SM (GSM) [5] and SSK (GSSK). In GSM more than one active antenna are used to transmit same information, in this case enabling GSM to enjoy same benefits of classical SM while increasing spectral efficiency. Another variant of SM is Enhanced Spatial Modulation (ESM) introduced in [6]. ESM tends to overcome constraint of spectral efficiency in SM, by using signal constellation points as a way of conveying information, ESM uses varying combination of antenna index mapping and signal constellation points as a means of

This work was funded by the Ministry of Education, Kenya through (AfDB Bank).

978-1-6654-1984-0/21/$31.00 ©2021 IEEE

transmitting information. For data enhancement, security and reduction in demodulation complexity multiple rank modulation (MRM) systems have been proposed in [7] , [8]. Recently in [9], [10], a novel scheme of improving data rates, security and reliability in wireless communication known as sequence modulation (SqM) was proposed. The SqM schemes include frequency sequence modulation, antenna code sequence and code word sequence modulation. In SqM schemes, information is conveyed through the sequence of elements at the transmitter.In [11], Pulse index Modulation (PIM) and Generalized PIM (GIPM) are proposed, in which they use Hermite-gaussian pulses shapes instead of antenna index for conveying information.This paper proposes use of mixed Gaussian channel in SqM to convey information by assigning transmit antenna channel patterns to incoming bits in SSK scheme.

Recently indexing mechanism concept has been greatly exploited, with the SM concept generalized to index modulation (IM). IM-aided schemes include Frequency domain (FD)-IM , Space Domain (SD)-IM, Time Domain (TD)-IM and Channel Domain (CD)-IM. In FD-IM also refereed to as IM-OFDM, additional information bits are conveyed by the indices of activated sub-carriers, as in [12] sub carrier-index modulated OFDM.In IM-TD, for a given data frame part of the signalling time-slots are activated for data transmission and corresponding inddices carry information [13], while CD-IM which is also reffered to as Medium based modulation (MBM), in this scheme which was first proposed in [14] utilizez variable channelstates for conveying information.Motivated by variety of ways in conveying information in literature for the IM-aided scheme, we propose SSK-ASM.

B. Contributions

In this paper, we propose a novel scheme employing SSK and antenna sequence for conveying information according to the incoming information bits. In contrast to classical SM and its variants, proposed SSK-ASM uses all three transmit antenna in a unique sequences for conveying information, therefore suitable for security sensistive based systems.

The main contributions are as below:

- We propose SSK-ASM for MIMO systems. Similiar to SSK, but with added security with odd transmit antennas.
- We formulate theoretical frame work by cleverly utilizing the classical SM-SIMO system for MQAM in developing ABEP for Maximum likelihood (ML) detector.
- We demostrate use ABEP analysis developed in [15] for use in SSK systems.
- Simulation results match well with developed ABEP for SSK-ASM

The rest of the paper is organized as follows: Section II presents the system model and mapper of SSK-ASM scheme. In section III, performance analysis of proposed scheme is presented. Performance comparison and simulation results are outlined in section IV and finally, the paper in concluded in section V.

Notation: Bold upper and lower case symbols denote matrices and scalar quantities respectively, and scalar quantities are represented as regular letters. The floor operation, is denoted by $\lfloor \cdot \rfloor$ and factorial operation by $(\cdot)!$ while $E[\cdot]$ denotes the expectation operator. $\|\cdot\|_F$ denotes the Frobenius norm operator, $(\cdot)^H$ denotes the Hermitian operator, $(\cdot)^\star$ denotes the conjugate operation and $(\cdot)^T$ denotes the transpose operation. We use $\binom{\cdot}{\cdot}$ to denote combination operation and $J_0(\cdot)$ denotes the zero-order Bessel function of the first kind.

II. SSK-ASM MODULATION

The SSK-ASM system model is given in Fig.1, which consists of a MIMO wireless link with three transmit antennas and Nr receive antennas. Incoming information bits b enters the SSK-ASM mapper, which groups $m = \log_2 2^{N_t+1}$ bits and maps them to known constellation vector $s_i^{(j)} = [s_i^{(1)} s_i^{(2)} s_i^{(3)}]^T$ according to mapping table given in Table I with unity power (i.e. $E_s[s^H s] = 1$). In SSK-ASM, only one antenna is active in a given time-slot during transmission, and hence only one entry of $s_i^{(j)}$'s in s is non-zero. The signal is transmitted over Flat Rayleigh Fading channel H and affected by addittive white Gaussian noise (AWGN) $\mathrm{n} = [n_1, n_2 \cdots n_{Nr}]^T$. Therefore the received signal during j^{th} time-slot is given by,

$\mathrm{r}^{(j)} = \mathrm{H}\mathrm{s}_{ij}^{(j)} + \mathrm{n}^{(j)}$, where n is independent and identically distributed (iid) entry as per $\mathcal{CN}(0,1)$. At the receiver, the ML-detector estimates the antenna indices that are used in each time-slot during transmission, and demaps the symbol to its component bits $\hat{\mathrm{b}}$ after all three estimates from time-slots are received. The table I shows mapping table for the proposed SSK-ASM, where $\mathrm{s_i}$ denotes the source channel from the antenna i ($\mathrm{s_i}$).Transmit antenna is arranged to transmit information through a pattern.

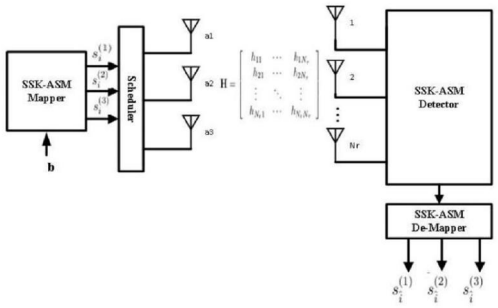

Fig. 1. SSK-ASM System Model.

TABLE I
SSK-ASM Mapper

Input bits b	Tx Antenna Source Channels: Time slot 1 $j=1$	Time slot 2 $j=2$	Time slot 3 $j=3$
0000	s_1	s_1	s_1
0001	s_1	s_1	s_2
0010	s_1	s_1	s_3
0011	s_1	s_2	s_2
0100	s_1	s_2	s_3
0101	s_1	s_3	s_2
0110	s_2	s_2	s_2
0111	s_2	s_2	s_1
1000	s_2	s_2	s_3
1001	s_2	s_1	s_1
1010	s_2	s_3	s_1
1011	s_2	s_1	s_3
1100	s_3	s_3	s_3
1101	s_3	s_3	s_1
1110	s_3	s_3	s_2
1111	s_3	s_2	s_2

TABLE II
SSK-ASM Transmission Example

b=[b_1 b_2 b_3 b_4]	Time-slot	j	$s_{ij} = [s_{i1}\ \ s_{i2}\ \ s_{i3}]^T$
[0 0 0 0]	1	1	$[1\ 0\ 0]^T$
	2	1	$[1\ 0\ 0]^T$
	3	1	$[1\ 0\ 0]^T$
[0 0 1 1]	1	1	$[1\ 0\ 0]^T$
	2	2	$[0\ 1\ 0]^T$
	3	2	$[0\ 1\ 0]^T$
[1 0 1 0]	1	2	$[0\ 1\ 0]^T$
	2	3	$[0\ 0\ 1]^T$
	3	1	$[1\ 0\ 0]^T$

A. SSK-ASM Transmission

The concept of SSK-ASM is using only antennas in a pattern to convey information. Unique pattern is used to convey information as per the table I. Hence, for the proposed SSK-ASM we use three antennas in a sequence to transmit 4 bits, but since three time slots are used then spectral efficiency (SE) 1.333 bits per channel use (bpcu), this advantegous since using three antennas in classical SSK and SM achievable SE is 1 bpcu. Suppose we transmit incoming bits [0000 0011 1010], m group of bits are transmitted according to the mapping table in Table I. So bits 0000 will be mapped to $[s_1\ \ s_1\ \ s_1]$ and transmitted as s_1 in timeslot one, and again s_1 in time slot 2 as illustrated in Table II, where i represent i^{th} active antenna in time-slot j^{th}.Hence, s_{ij} specifies an N_j-dimesional vector, where N_j known modulation symbols are each transmitted via time slot j, $j \in [1 : N_j]$, for example, active antenna one in time-slot one is given as $s_{ij} = [s_{i1}\ \ 0\ \ 0]^T$.The symbols s_{ij} in Table II are known and equal, i.e., $\mathrm{s}_{ij} = s_{i1} = s_{i2} = s_{i3}$.

B. SSK-ASM Detection

The ML-detector obtains the antenna indices for a given time-slot as used at the transmitter. Assuming equally likely channel inputs, the ML-detector is given as,

$$\begin{aligned} s_{ij}^{(j)} &= \arg\max p_R(\mathrm{r}^{(j)}|\mathrm{s}_{ij}^{(j)}, \mathrm{H}) \\ &= \arg\min \left[\|\mathrm{g}_{ij}^{(j)}\|^2 - 2\Re(\mathrm{r}^{(i)H}\mathrm{g}_{ij}^{(j)})\right] \end{aligned} \tag{2}$$

where $\mathbf{g}_{ij}^{(j)} = \mathbf{h}_j^{(j)} s_i$, $j \in [1 : N_j]$, $i \in [1 : M]$ and the conditional probability density function (PDF) of r given H and s_{ij} for a single SSK-ASM stream is written as,

$$p_R(\mathrm{r}^{(j)}|\mathrm{s}_{ij}^{(j)}, \mathrm{H}) = \pi^{-N_r} \exp(- \parallel \mathrm{r}^{(j)} - \mathrm{H}\mathrm{s}_{ij}^{(j)} \parallel_F^2) \tag{3}$$

III. PERFORMANCE ANALYSIS

A. Equivalent symbol error probability

The performance of the SSK-ASM system is derived using the previous study on multiple active-spatial modulation (MA-SM) system introduced performance analysis of SM systems using a single equation for error probability [15]. Here we apply intuitively a similar approach to analyze the SSK-ASM system. The approach uses the well-known error analysis of a single-input multiple-output (SIMO) system to derive the probability of bit error for various SM systems. A principle is used where equivalent number of bits in error is derived from mutual information (MI) and sample variance (SV) criteria and used to obtain the probability of bit error jointly for both the spatial and modulation domains.For a conventional SIMO system, the exact symbol error probability (SEP) for square M-ary MQAM is given as [16]

$$P_{s-SIMO}(e|\bar{\gamma}) = aQ\left(\sqrt{\frac{b\bar{\gamma}}{N_a}}\right) - 4a^2Q^2\left(\sqrt{\frac{b\bar{\gamma}}{N_a}}\right) \tag{4}$$

where, $a = (1 - \frac{1}{\sqrt{M}})$, $b = (\frac{3}{M-1})$, $Q(\zeta)$ and $Q^2(\zeta)$ are first and second craig's equations given by $Q(\zeta) = \frac{1}{\pi}\int_0^{\frac{\pi}{2}} \exp\left(-\frac{\zeta^2}{2\sin^2\theta}\right) d\theta$, and $Q^2(\zeta) = \frac{1}{\pi}\int_0^{\frac{\pi}{4}} \exp\left(-\frac{\zeta^2}{2\sin^2\theta}\right) d\theta$ respectively. The craig's equations can be approximated to a summation problem through composite trapezoidal rule, then the SEP in (4) can be simplified as,

$$\begin{aligned} P_{s-SIMO}(e|\bar{\gamma}) = \frac{a}{z}\left[\frac{1}{2}\exp(-\frac{b\bar{\gamma}}{2}) - \frac{a}{2}\exp(-b\bar{\gamma})\right] \\ + \frac{a}{z}\left[(1-a)\sum_{i=1}^{z-1}\exp(-\frac{b\bar{\gamma}}{S_i}) + \sum_{i=z}^{2z-1}\exp(-\frac{b\bar{\gamma}}{S_i})\right] \end{aligned} \tag{5}$$

where z refers to the number of iterations used in the approximation and $S_i = 2\sin^2(\frac{\pi i}{4z})$.

The computation of the P_{s-SIMO} can be further simplified through moment generating functions (MGF) [17]. The transmitted symbol error rate (SER), P_s is equivalent to the average SER of square-QAM with MRC reception over i.i.d fading channels for (MQAM) modulation. From MA-SM, the expanded form of the SIMO SEP is given as the conventional modulation signal under ML detection, thus,

$$P_{s-SIMO} = \frac{a}{z}\left[\frac{1}{2}\prod_{k=1}^{N_r}\left(\frac{2}{b\bar{\gamma_k}+2}\right) - \frac{a}{2}\prod_{k=1}^{N_r}\left(\frac{1}{b\bar{\gamma_k}+1}\right)\right] + \frac{a}{z}\left[(1-a)\sum_{i=1}^{z-1}\prod_{k=1}^{N_r}\left(\frac{S_i}{b\bar{\gamma_k}+S_i}\right) + \sum_{i=z}^{2z-1}\prod_{k=1}^{N_r}\left(\frac{S_i}{b\bar{\gamma_k}+S_i}\right)\right] \tag{6}$$

The expression in (6) gives the SIMO MQAM SEP for correlated Rayleigh channels, where a minimal summation value of $z = 20$ is sufficient.

B. Joint Antenna and Symbol probability of error

Given that the overall SEP for SM system, P_{S-SM} is known, then the bit error probability (BEP) may simply be written as $P_B \leq \frac{P_{S-SM}}{b_{max}}$,where b_{max} is the total number of conveyable bits in SM [3]. Then, the BEP for SM system may be re-written as,

$$\begin{aligned} P_B &= \frac{P_{S-SM}}{b_{max}} \\ &= \frac{P_{S-SM}}{b_{max}} v_e \\ &= \frac{P_S}{b_e} \end{aligned} \tag{7}$$

where v_e denotes the coefficient of increase in error above that of a SIMO space and $b_e = \frac{b_{max}}{v_e}$ is the density of bits in error for an equivalent SIMO system. The problem is to deduce the principal components in the joint space, which will be equivalent to be bits.

C. Effective density of bits in error for ASM

SSK-ASM system waits for the 3 timeslots before demapping the conveyed information. Therefore, the detection errors will increase and are linearly dependent on the number of transmit chains N_a in the multiplexing space [15]. Accordingly, since each element of the covariance matrix is computed between any two data components; the number of covariance samples I_c in the combined space for ASM can be computed as [15],

$$I_c = \binom{N_a}{2} = \frac{N_a!}{2!(N_a-2)!} \tag{8}$$

Since there are N_a chains in the 3 timeslots, the spatial space is thus expanded from N_t to $I_c N_t$ for each covariance stream and this expansion in space reduces the number density by $I_c N_t$, hence increase in error. Consequently, following SV criterion, we can re-write the density of bits in ASM as,

$$b_{e,SV} = \frac{1}{I_c \times \sqrt{\frac{I_c N_t}{M-1}}} \tag{9}$$

Similarly, following MI criterion, we have $q(x) = \frac{1}{I_c N_t}$, while $p(x)$ remains the same as $p(x) = \frac{1}{M-1}$ and consequently we have,

$$b_{e,MI} = \left|\log_2\left(\frac{I_c N_t}{M-1}\right)\right| \tag{10}$$

For example, in the case $I_c = 1$, conforms to SM. However, the signal from the symbol modulation space is always known.As a result, in order to select the best model, the criterion that gives the minimum number of bits in error will be selected. Thus, we have

$$b_{e(ASM)} = \min(b_{e,SV}, b_{e,MI}) \tag{11}$$

D. Overall Bit Error Rate for SSK-ASM

The expression in (11) can then be used together with (7) and (8) to compute the BEP for SSK-ASM system as the ratio of the symbol error, P_S and the effective number of bits, b_e being the average lower bound error. The average probability of bit error is estimated as follows,

$$\begin{aligned} P_B &= \frac{P_S}{b_{e(ASM)}} \\ &= P_{SSK-ASM} \end{aligned} \tag{12}$$

Estimation of the SSK-ASM error can be evaluated as the difference in error from a joint ASM error and conventional MQAM error. Let 4QAM be used to transmit the signal under ASM. Therefore, the error for SSK-ASM will be the difference between ASM and conventional bit error for 4QAM, i.e.

$$P_{SSK-ASM} = \left[\frac{P_S^{4QAM}}{b_{e(ASM)}} - \frac{\eta_e P_S^{4QAM}}{\log_2(M)}\right] \tag{13}$$

where η_e refers to the number of unique error sources for the three timeslots. These error sources are equal to the unique patterns in which the transmit antennas are used in each timeslot.As a result, the SSK-ASM system has $\eta_e = 8$. For the case of SSK-ASM, the following parameters are used to derive error probability: $N_a = 3, I_c = 3, N_j = 3, M = 4$ and $\eta_e = 8$, where η_e is the number of all possible sequence patterns at the detector.

IV. SIMULATION RESULTS

To show performance of the proposed scheme, the BER os SSK-ASM is evaluated. The classical SSK is used as a benchmark. The signal-to-noise ratio (SNR) used in simulations is defined as $\frac{E_s}{N_0}$ where E_s is energy per unit symbol and N_0 as noise power. ML detector is assumedat the reciever for simulated systems.Source channel used in proposed scheme is flat Rayleigh fading channel. Fig. 2 shows the theoretical and simulation ABEP performance

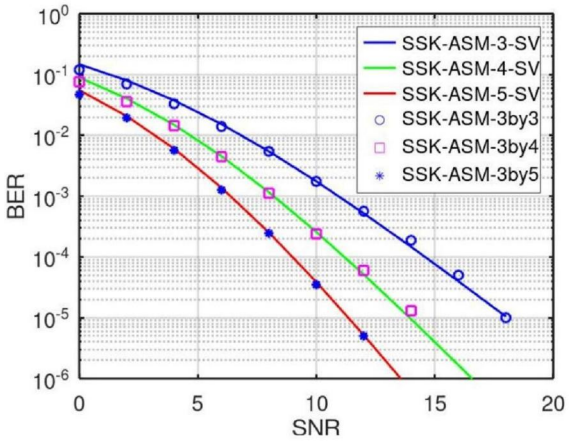

Fig. 2. BER of SSK-ASM at 1.333 bpcu with $N_r = 3, 4, 5$.

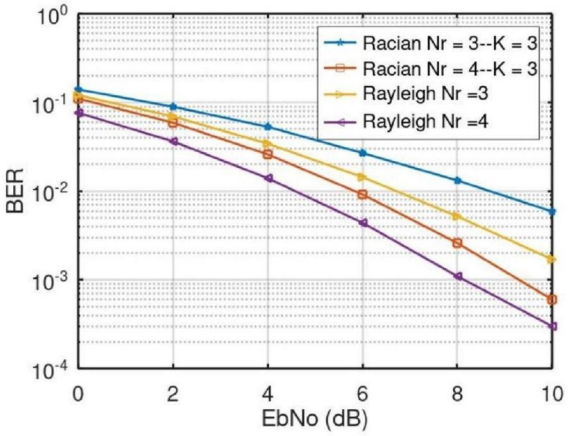

Fig. 4. SSK-ASM under Rayleigh and Racian Channels.

plots with SSK-ASM with $Nr = 3, 4, 5$ for SV criteria.The channel considered is Rayleigh Flat fading in the pattern sequences. As can onbserved from the Fig. 2, the analytical and simulation results match well throughout the SNR range.

Furthermore, Fig. 3 depitcs BER results obtained for SSK-ASM with four receive antennna and compared with classical SSK 3 by 4 system. At 10^{-4}BER, the proposed scheme requires 1dB extra power compared to classical SSK, although the proposed scheme can achieve additional 1.333 bpcu for the same number of antennas of SSK.
Further simulations was done as shown in Fig. 4, depicting performance of SSK-ASK under Rayleigh compared to Racian channel, bad channel Rayleigh was shown to perform better than the good Racian channel, this is due to the fact that since channels are solely used to convey information hence less error detections to a more scattered channel than less scattered.

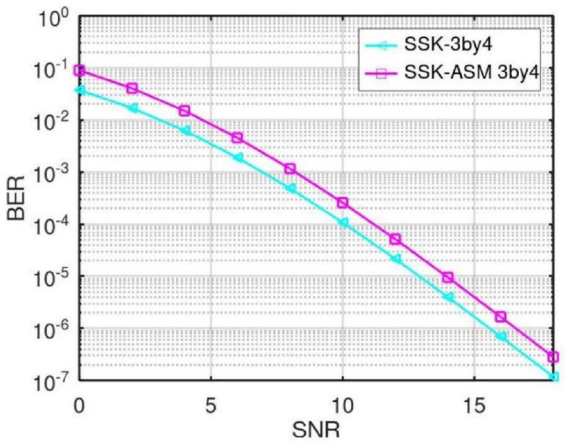

Fig. 3. BER comparisons of SSK and SSK-ASM, where $N_r = 4$.

V. CONCLUSIONS

We have proposed a new SSK based scheme - SSK-ASM, which exploit the both antenna indices and pattern in conveying information. This method is able to accomodate odd number of antenna in transmission and additional SE of 1.333 bpcu than that of SSK.Analytical expressions for average BER of the SSK-ASM scheme have been derived and was tightly bound to simulations.This scheme due to its uniqueness of the antenna pattern can enhance security to the IM based systems.

References

[1] P. Wolniansky, G. Foschini, G. Golden, and R. Valenzuela, "V-BLAST: an architecture for realizing very high data rates over the rich-scattering wireless channel," in Proc. ISSSE-98, Pisa, Italy.

[2] State of the IoT 2020: 12 billion IoT connections, surpassing non-IoT for the first time, Accessed on: Jan. 3, 2021.

[3] R. Y. Mesleh, H. Haas, S. Sinanovic, C. W. Ahn, and S. Yun, "Spatial modulation," IEEE Trans. Veh. Technol., vol. 57, no. 4, pp. 2228–2241, 2008.

[4] J. Jeganathan, A. Ghrayeb, L. Szczecinski and A. Ceron, "Space shift keying modulation for MIMO channels," IEEE Transactions on Wireless Communications, vol. 8, p. 3692–3703, 2009.

[5] A. Younis, N. Serafimovski, R. Mesleh and H. Haas, "Generalised spatial modulation," in 2010 conference record of the forty fourth Asilomar conference on signals, systems and computers, 2010.

[6] C.-C. Cheng, H. Sari, S. Sezginer and Y. T. Su, "Enhanced spatial modulation with multiple signal constellations," IEEE Transactions on Communications, vol. 63, p. 2237–2248, 2015.

[7] Peter Akuon and Hongjun X."A multiple Rank Modulation System" US Patent 2018/0269944 A1, 2018.

[8] Nyawade, A., Akuon, P. O., Xu, H., Kalecha, V. O., 'Spatial MIMO Rank Modulation,' IEEE AFRICON, 2019, Accra, Ghana.

[9] Akuon, P. O., 'Frequency Sequence Modulation: Analysis of additional Spectrum Space,'IEEE AFRICON, 2019, Accra, Ghana.

[10] Akuon, P. O., Xu, H., 'Sequence Modulation: Genetically-inspired Transmission of Information,'SATNAC 1-4 Sept 2019, Durban, S. Africa, pp.1-4.

Q-Function: Trapezoidal Rule Approximation and Application.

Abdulrahman A. Faris*, Peter O. Akuon*,
*School of Engineering, University of Nairobi
Nairobi, Kenya
abdulrahman@uonbi.ac.ke , akuon@uonbi.ac.ke

Abstract— **In this paper, we systematically present numerical approximation of Gaussian error integral, Q-function using trapezoidal rule and its application to performance analysis of Binary-Phase -Shift -Keying and M-QAM modulation schemes. Moreover, the close form derived of symbol error rate (SER) are then compared with different Gaussian Q-function approximation available from literature.**

Index Terms — **BPSK, Q-function, error function, , trapezoidal rule.**

I. INTRODUCTION

The Gaussian Q-function *Q(x)* and complementary error function *erfc(x)* are of great significance in digital communication systems modelling. The *Q(x)* and *erfc(x)* are widely available as function routines in a various mathematical modelling software, such as MATLAB. However, close form or approximation are useful in performance analysis of communication theory.

The Gaussian error function or Q-function which is defined in [1] as complement cumulative distribution function (CDF) of Gaussian random variable (RV) and given as:

$$Q(x) = \frac{1}{\sqrt{2\pi}} \int_x^{\infty} exp\left(\frac{-\beta^2}{2}\right) d\beta \qquad (1)$$

The above presentation of Q-function is the classical form, which cannot be solved analytically because of two drawbacks [1]:

(i). presence of infinite upper limit, and

(ii). lower limit as a variable of the function argument.

Hence the need of alternate form, which is tight and simple in manipulation analytically cannot be overemphasized.

The rest of the paper is laid down as follows: section II discusses alternate form of (1) and its various approximation in literature. Section III, approximation of Q-function using trapezoidal rule is presented with application to BPSK and under AWGN and over Rayleigh fading, and in section IV comparison with Monte Carlo simulation. Section V concluding remarks.

II. Q-Function Approximations

Although the existence of (1) traced back to Nuttal's report of 1972 [2], it is after two decades that it gained fame from the craigs work [3] by formulating an alternate form known as craig's formula given as:

$$Q(x) = \frac{1}{\pi} \int_0^{\frac{\pi}{2}} exp\left(-\frac{x^2}{2sin^2\theta}\right) d\theta \qquad (2)$$

Alternative derivations of (2) can be found in [4]. The *Q(x)* and *erfc(x)* are related by [5]

$$Q(x) = \frac{1}{2} erfc\left(\frac{x}{\sqrt{2}}\right) \qquad (3)$$

In [6] , *Q(x)* is approximated in terms of *erfc(x)*, using (3) is given as a sum of two exponential,

$$Q(x) \approx \frac{exp\left(\frac{-x^2}{2}\right)}{12} + \frac{exp\left(\frac{-2x^2}{3}\right)}{4} \qquad (4)$$

The approximation (4) is suited for some applications, but not tightly bound on large errors over small arguments, hence confines its application [7], and another approximation presented by Karagiannidis & Lioumpas [8] gives an improvement of (4) and has smaller error approximation given as,

$$f(x, A, B) = \frac{(1 - exp^{-Ax}) exp^{-x^2}}{B\sqrt{\pi x}} \approx erfc(x) \qquad (5)$$

where A= 1.98, and B=1.135.

but an argument in the denominator of (5) poses difficulty in evaluation the probability of error [9]. Other approximations include from works of Kingsbury [10] and Chernoff bound [11] presented as equation (6) and (7) respectively. Most recently approximation to best of my

knowledge is by [12], using Maclaurin-Taylor series expansion of error function *erf(x),* (8),

$$Q(x) \approx \frac{exp\left(-\frac{x^2}{2}\right)}{1.64 + \sqrt{0.76x^2 + 4}} \quad (6)$$

$$Q(x) \approx \frac{1}{2} exp\left(-\frac{x^2}{2}\right) \quad (7)$$

$$Q(x) \approx \frac{1}{2} + \sum_{n=1}^{n_a} A_n x^{2n-1} \quad (8)$$

Where A_n is given as,

$$A_n = \frac{(-1)^n}{\sqrt{\pi} 2^{\left(\frac{2n-1}{2}\right)} (n-1)!\,(2n-1)} \quad (9)$$

The complexity and limitations of the aforementioned approximations, necessitated our presentation of composite trapezoidal rule (10) for approximation of Gaussian error integral of craigs' form. The approximation of $Q(x)$ and $Q^2(x)$ follows;

$$\int_a^b f(x)dx = \frac{b-a}{N}\left[\frac{f(a)+f(b)}{2} + \sum_{k=1}^{N-1} f\left(a + k\frac{b-a}{N}\right)\right] \quad (10)$$

Using (10) on (2), $Q(x)$ can approximated to (11), with N being number of iterations.

$$Q(x) = \frac{1}{2N}\left[\frac{exp\left(\frac{-x^2}{2}\right)}{2} + \sum_{k=1}^{N-1} exp\left(\frac{-x^2}{2sin^2\theta_k}\right)\right] \quad (11)$$

and by using craigs second formula (12) on (2), $Q^2(x)$ can approximated as (13)

$$Q^2(x) = \frac{1}{\pi}\int_0^{\frac{\pi}{4}} exp\left(-\frac{x^2}{2sin^2\theta}\right) d\theta \quad (12)$$

$$Q^2(x) = \frac{1}{4M}\left[\frac{exp(-x^2)}{2} + \sum_{k=1}^{M-1} exp\left(-\frac{x^2}{2sin^2\beta_k}\right)\right] \quad (13)$$

where $\theta_k = \frac{k\pi}{2N}$, $\beta_k = \frac{k\pi}{4M}$ and N, M are number of iterations. Figure1, shows plot of Q-function approximation and MATLAB 'qfunc' function.

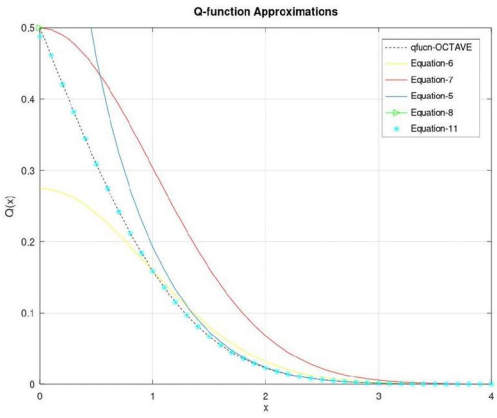

Figure 1: Comparison (6)-(8), (11) against 'qfunc'

III. APPLICATION

BPSK Analysis Under AWGN

The performance metrics of communication system, symbol error rate (SER), are expressed in terms of Q-function and available in various literature such as [13, Table 4.3]. SER of BPSK under AWGN is given as ,

$$P_{eBPSK} = Q\left(\sqrt{2\gamma}\right) \quad (14$$

where $\gamma = \frac{E_S}{N_O}$

$$P_{eMQAM} = aQ\left(\sqrt{b\gamma}\right) - \left(\frac{a}{2}\right)^2 Q^2\left(\sqrt{b\gamma}\right)$$

where $a = 4\left(1 - \sqrt{1/M}\right)$, $b = \frac{3}{M-1}$

Using (7) SER of BPSK can be expressed as,

$$Q\left(\sqrt{2\gamma}\right) = \frac{1}{2N}\left[\frac{exp(-\gamma)}{2} + \sum_{k=1}^{N-1} exp\left(\frac{-\gamma}{sin^2\theta_k}\right)\right] \quad (15)$$

and SER from different approximations equation (4) – (8) are tabulated in table 1.

The presented approximations were compared with monte Carlo simulation of BPSK under AWGN and results are shown in figure 2. The number of iterations used in (8) and (15) are two and five respectively. Approximation (15) follows simulation tightly. For (8) to have low error, n_a needs to be greater than forty [12].The lack of exponential in (8) make it difficult in performance analysis of wireless communication systems under fading which require averaging over distribution function,

which will need truncation of the upper infinite limit when averaging, hence the excellence of (11).

Table 1

Approx.	SER- BPSK
4	$\frac{exp(-\gamma)}{12}+\frac{exp\left(\frac{-4\gamma}{3}\right)}{4}$
5	$Q(x)\approx\frac{\left(1-\frac{1}{\sqrt{2}}exp(-Ax)\right)exp\left(-\frac{x^2}{2}\right)}{B\sqrt{2\pi}x}$
6	$\frac{exp(-\gamma)}{1.64+\sqrt{1.52\gamma+4}}$
7	$\frac{1}{2}exp(-\gamma)$
8	$\frac{1}{2}+\sum_{n=1}^{n_a}A_n\left(\sqrt{2\gamma}\right)^{2n-1}$

BPSK Analysis Over Fading

Here we present close-form expression of SER for BPSK under Rayleigh fading using MGF method. the exact SER of BPSK under fading is given as (16) in [14, A.5].

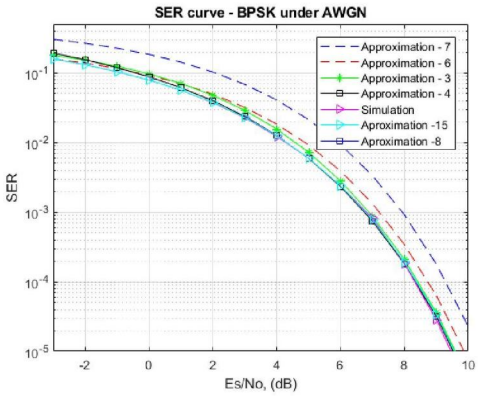

Figure 2 Results for BPSK under AWGN using Approximations and Monte Carlo Simulation

Using (15) and averaging over Rayleigh distribution, and after manipulation we arrive to (17) as SER of BPSK over fading using our proposed approximation, comparison with simulation is shown in figure 3.

$$P_{eBPSK}=\frac{1}{4N}\left[\frac{1}{1+\gamma}\right]+\frac{1}{2N}\left[\frac{s_n}{s_n+\gamma}\right] \quad (16)$$

where $s_n=sin^2\theta_n \quad \theta_n=\frac{n\pi}{2N}$

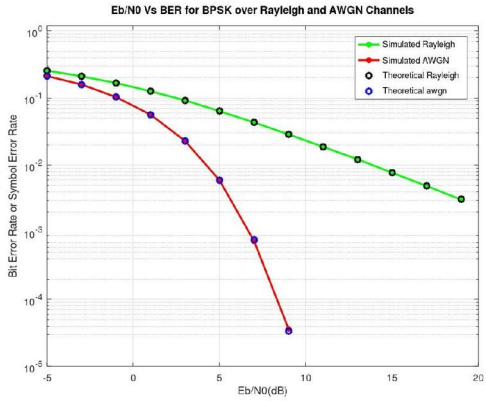

Figure 3 Results for BPSK Rayleigh fading using Equation 17 and Monte Carlo Simulation

VI. CONCLUSION

The composite trapezoidal rule was used in this paper to formulate closed-form expression of Craig's first and second equation. The proposed expression was applied to derive close-form expression of SER for BPSK under AWGN and fading. The closed-form is simple and can easily be manipulated to formulate probability of error under fading by using moment generating function (MGF).

REFERENCES

[1] Simon, Marvin K., 'Probability Distributions Involving Gaussian Random Variables A Handbook for Engineers and Scientists', Springer, 2006.

[2] A. Nuttall, "Some integrals involving the Q-function," Naval Underwater Systems Center, New London, CT, Tech. Rep. 4297, Apr. 17, 1972. https://apps.dtic.mil/dtic/tr/fulltext/u2/743066.pdf

[3] J. W. Craig, "A new, simple and exact result for calculating the probability of error for two-dimensional signal constellations," MILCOM 91 - Conference record, McLean, VA, USA, 1991, pp. 571-575 vol.2, doi: 10.1109/MILCOM.1991.258319.

[4] Stewart, Seán. (2017). Some alternative derivations of Craig's formula. The Mathematical Gazette. 101. 268-279. 10.1017/mag.2017.66.

[5] M. K.Simon and M.S. Alouini, Digital communications over fading channels: A unified approach to performance analysis, John Wiley & Sons, 2000.

[6] R. Nicole, "New exponentional bounds and approximations for the computation of error probability in fading channels," IEEE Trans. Wireless Commun., vol.2, pp.840-845, Jul. 2003.

[7] Malluri, Sirisha & Pamula, Vinay Kumar. (2013). Gaussian Q-function and Its Approximations. 74-77. 10.1109/CSNT.2013.25.

[8] G.K. Karagiannidis and A.S.Lioumpas, "An improved approximation for the Gaussian Q-function," IEEE Commun. Lett., vol. 11, no. 8, pp. 644–646, Aug. 2007.

[9] Y. R. B. Isukapalli, "An Analytically Tractable Approximation for the Gaussian Q-Function," IEEE Communications Letters, vol.12, no.9, pp.669-671, Sep. 2008.

[10] N. Kingsbury, "Approximation formulae for the Gaussian, error integral," work produced by the connexions project. Available: http://cnx.org/content/m11067/latest/
[11] M. Ambramowitz and I.A. Stagun, "Handbook of Mathematical functions with formulas, graphs and mathematical tables," p.257, 940, 941, National bureau of standards, 1964.
[12] ShirinAbadi, Parnian & Abbasi, Arash. (2019). On Approximation of Gaussian Q-Function and its Applications. 0883-0887. 10.1109/UEMCON47517.2019.8992958.
[13] Zhang, K.Q. (2015). Digital Modulation. In Wireless Communications, K.Q. Zhang (Ed.). doi:10.1002/9781119113263.ch4
[14] **Yang**, Sung-Moon Michael, 'Modern Digital Radio Communication Signals and Systems',Springer,2019.

APPENDIX B: Tables of Results

Table 5.1: SSK-SqM BER Performance using MI criteria.

BER of SSK-SqM with $N_{RX} = 3, 4, 5$ - MI Criteria						
Theory - MI Criteria				**Simulation**		
dB	$N_{RX} = 3$	$N_{RX} = 4$	$N_{RX} = 5$	$N_{RX} = 3$	$N_{RX} = 4$	$N_{RX} = 5$
0	0.41587	0.25321	0.1564	0.12	0.076	0.047
2	0.22628	0.11406	0.058453	0.07	0.036	0.0194
4	0.10618	0.042134	0.017035	0.033	0.0145	0.00567
6	0.043118	0.012814	0.0038871	0.014	0.00448	0.001267
8	0.015401	0.0032767	0.00071267	0.00544	0.00112	0.000245
10	0.0049553	0.00072729	0.00010924	0.00175	0.00024	3.50E-05
12	0.0014731	0.00014498	1.46E-05	0.000567	6.00E-05	5.00E-06

Table 5.2: SSK-SqM BER Performance using SV criteria.

BER of SSK-SqM with $N_{RX} = 3, 4, 5$ - SV Criteria						
Theory - SV Criteria				**Simulation**		
dB	$N_{RX} = 3$	$N_{RX} = 4$	$N_{RX} = 5$	$N_{RX} = 3$	$N_{RX} = 4$	$N_{RX} = 5$
0	0.14765	0.089899	0.055529	0.12	0.076	0.047
2	0.080337	0.040495	0.020753	0.07	0.036	0.0194
4	0.037697	0.014959	0.0060482	0.033	0.0145	0.00567
6	0.015309	0.0045494	0.0013801	0.014	0.00448	0.001267
8	0.005468	0.0011634	0.00025303	0.00544	0.00112	0.000245
10	0.0017593	0.00025822	3.88E-05	0.00175	0.00024	3.50E-05
12	0.00052299	5.15E-05	5.19E-06	0.000567	6.00E-05	5.00E-06

Table 5.3: BER: Flat Fading Channels - Uncorrelated.

Flat Fading Channels - Uncorrelated							
Rayleigh				**Rician** $N_{RX} = 3$		**Rician** $N_{RX} = 4$	
dB	$N_{RX}3$	$N_{RX}4$	$N_{RX}5$	$K = 3$	$K = 10$	$K = 3$	$K = 10$
0	0.1206	0.0764	0.0485	0.1583	0.1327	0.1106	0.0867
2	0.0696	0.0364	0.0189	0.0996	0.0791	0.0591	0.0429
4	0.0343	0.0140	0.0058	0.0546	0.0403	0.0260	0.0175
6	0.0144	0.0044	0.0013	0.0253	0.0173	0.0092	0.0056
8	0.0052	0.0011	0.0003	0.0101	0.0066	0.0101	0.0066
10	0.0017	0.0003	0.0000	0.0035	0.0022	0.0035	0.0022
12	0.0005	0.0001	0.0000	0.0011	0.0006	0.0011	0.0006
14	0.0001	0.0000	0.0000	0.0003	0.0002	0.0003	0.0002

Table 5.4: BER: Flat Fading Channels - Correlated.

Flat Fading Channels - Correlated								
Rayleigh					**Rician**			
$d = 0.1\lambda$			$d = 0.5\lambda$		$d = 0.1\lambda$		$d = 0.5\lambda$	
dB	$N_{RX}3$	$N_{RX}4$	$N_{RX}3$	$N_{RX}4$	$N_{RX}3$	$N_{RX}4$	$N_{RX}3$	$N_{RX}4$
0	0.1635	0.1191	0.1132	0.0713	0.1992	0.1545	0.1384	0.089
2	0.1139	0.0743	0.0645	0.0339	0.1448	0.1013	0.0821	0.0443
4	0.076	0.043	0.032	0.0133	0.096	0.0619	0.0433	0.0177
6	0.0416	0.0212	0.0136	0.0042	0.0595	0.0342	0.0189	0.0062
8	0.0222	0.0105	0.0049	0.0011	0.0334	0.0166	0.0075	0.0019
10	0.0111	0.0044	0.0016	0.0003	0.0171	0.008	0.0027	0.0005
12	0.0048	0.0018	0.0005	0.00005	0.0079	0.0035	0.001	0.0001

Table 5.5: BER - SSK-SqM Vs. ASM.

BER - SSK-SqM Vs. ASM-$N_{RX} = 3$				
	SSK-SqM	**ASM**		
dB		**dB**	**4-QAM**	**BPSK**
0	0.12114	0	0.25	0.15
3	0.04972	2	0.18	0.1
6	0.01408	4	0.1	0.05
9	0.002955	6	0.05	0.022
12	0.000526	8	0.02	0.008
15	7.40E-05	10	0.007	0.0027
18	9.00E-06	12	0.002	0.0008

Table 5.6: BER - SSK-SqM Vs. 4QAM, SM and SSK.

BER - SSK-SqM Vs. (4QAM, SM and SSK)$N_{RX} = 4$				
dB	4QAM	SSK_SqM	SM	SSK
0	0.17828	0.076	0.09	0.037578
2	0.10199	0.036	0.045	0.016927
4	0.04618	0.0145	0.02	0.006253
6	0.015548	0.00448	0.0065	0.0019017
8	0.0049683	1.12E-03	0.0018	0.00048629
10	1.12E-03	2.40E-04	0.0004	0.00010794
12	2.14E-04	6.00E-05	0.00008	2.15E-05
14	3.83E-05	1.30E-05	0.000016	3.97E-06

Table 5.7: SSK-SqM Secrecy Rate.

Half Sequence Known to Eve - at various dB									
$N_{RX} = 3$				$N_{RX} = 4$			$N_{RX} = 5$		
dB	0-dB	3-dB	20-dB	0-dB	3-dB	20-dB	0-dB	3-dB	20-dB
0	0.122	0.003	-0.407	0.182	-0.05	-0.31	0.177	-0.08	-0.23
5	0.399	0.279	-0.133	0.436	0.204	-0.058	0.383	0.13	-0.025
10	0.513	0.394	-0.016	0.492	0.259	-0.0031	0.408	0.154	-0.0006
15	0.528	0.409	-9.3E-04	0.494	0.262	-6.9E-05	0.408	0.155	-4.7E-06
20	0.529	0.410	7.3E-05	0.494	0.2623	1.7E-06	0.408	0.155	3.8E-08
25	0.529	0.410	1.2E-04	0.494	0.2623	2.8E-06	0.408	0.155	6.3E-08
30	0.529	0.410	1.2E-04	0.494	0.2623	2.8E-06	0.408	0.155	6.3E-08
35	0.529	0.410	1.2E-04	0.494	0.2623	2.8E-06	0.408	0.155	6.3E-08

Table 5.8: Secrecy Rate SSK-SqM vs. SSK and SIMO

Half Sequence Known to Eve - at various dB with $N_{Rx} = 3$							
SSK-SqM			SIMO		Classical SSK		
dB	0-dB	3-dB	0-dB	3-dB	dB	0-dB	3-dB
0	0.1219	0.0028209	0	-0.12109	0	0	-0.20136
5	0.3985	0.27942	0.18043	0.059345	4	0.15364	-0.047716
10	0.51328	0.3942	0.24034	0.11925	8	0.22794	0.026584
15	0.52833	0.40925	0.24752	0.12643	12	0.24534	0.043978
20	0.52933	0.41025	0.24797	0.12689	16	2.48E-01	0.046373
25	0.52938	0.41029	0.24799	0.12691	20	2.48E-01	0.046614
30	0.52938	0.4103	0.24799	0.12691	24	2.48E-01	0.046635